ISSN: 0974-5823

International Journal of Mechanical Engineering

Volume No. 9
Issue No. 1
January - April 2024

ENRICHED PUBLICATIONS PVT. LTD

S-9, IInd FLOOR, MLU POCKET,
MANISH ABHINAV PLAZA-II, ABOVE FEDERAL BANK,
PLOT NO-5, SECTOR-5, DWARKA, NEW DELHI, INDIA-110075,
PHONE: - + (91)-(11)-47026006

ISSN: 0974-5823

International Journal of Mechanical Engineering

Aims and Scope

The "International Journal of Mechanical Engineering" is an peer reviewed journal. The goal of this journal is to provide a platform for academicians, researchers and practitioners all over the world to promote, share, and discuss various new issues and developments in all areas of Mechanical Engineering. Manuscripts are subject to a rigorous and fair peer-review process. Accepted papers will appear online within 3-4 weeks after their submission. The journal publishes papers including but not limited to the following topics:

ISSN: 0974-5823

International Journal of Mechanical Engineering

(Volume No. 9, Issue No. 1, Jan - Apr 2024)

Contents

Seismic Behavior of Schwedler Domes

1Asmaa Falih Dakheel, 2Dr. Ihab Sabri Saleh
1,2 Civil Engineering Department, College of Engineering, University of Basrah, Basrah, Iraq.

A B S T R A C T

Dome structures have been used extensively for long-span systems in industrial, residential, and military infrastructures for their ability to cover large areas without intermediate supports, their lightweight, and their splendid aesthetic appearance. The seismic behavior of such structures not only is directly related to the safety of a building but also has a huge influence on the safety of people. Therefore, it is necessary to understand the seismic behavior for these structures under seismic loads. In this study, the seismic behavior of single-layer steel reticulated spherical Schwedler dome subjected to three-directional earthquake ground motion was investigated. Two types of Schwedler domes were chosen for the analysis and design, Schwedler monoclinal dome (A-dome) and Schwedler bidirectional dome (B-dome). The finite element models were established using SAP2000 software version 24, fifty-four dome models resting on the earth with 60m span and rigid joints and having different geometric properties, including varying rise-to-span ratios (10, 20, and 30%), number of ribs, and number of latitudinal rings were studied. The models were designed only for gravity loads, and then the natural vibration properties were studied, after that the seismic load was applied. The seismic performance of Schwedler dome models is analyzed based on linear time history analysis (LTH); and the dynamic responses have been investigated. The results show that A and B dome models have identical vibration modes and dynamic responses, and the rise-to-span ratio has great influence on the dynamic characteristics, the rise-to-span ratio of 30% is the most suitable ratio for height of Schwedler domes with 60m span among the three ratios (10, 20, and 30%). In general, Schwedler domes can efficiently resist seismic loads.

Keywords: dynamic strength failure; failure mechanism; severe earthquake; reticulated domes, Schwedler dome

1. Introduction

The increasing demands of lighter, stronger and cheaper structures have prompted many architects, scientists, engineers to seek new technology and building concepts to achieve these goals [1]. The recent researches focus on structural systems that derive their performance from their curved shape, dictated by the flow of forces [2]. These structures can be extremely thin, elegant, cost-effective, earth-friendly, and have a smaller carbon footprint, that is because of their ability to cover large spans with a small amount of construction material and their effective structural characteristics [3-5]. There are many literatures which studied domes from different structural and geometrical aspects. Sabri and Abdulzahra [6] studied the response of space steel double layers frames with different positioning of point loads using Time History Analysis. Salih et al.[7] investigated the structural behavior of orthogonal square pyramid space grid under dynamic load, in which pyramid units with a square base are used. Jasim et al [8] studied the linear stresses and deformations of ribbed dome. Saleb and Muhsen [9] proposed several types of ribbed

domes to improve their resisting for seismic loads. Yu et al. [10] performed a research on failure mechanism of single-layer steel reticulated domes with the reinforced concrete substructure subjected to sever earthquakes. Ma et al. [11] investigated the dynamic behavior and a seismic design method for single-layer reticulated domes with semi-rigid joints. Valibeig et al. [12] examined the structural details of discontinuous double-shell domes and revealed the factors affecting them. Kaveh et al. [13] developed an algorithm for optimum design of domes considering the topology, geometry, and size of member section using the cascade-enhanced colliding bodies optimization method. In large-scale space steel structures, a large number of design variables are involved. Yan et al. [14] presented a method to identify the most critical member in a single-layer latticed dome, which in the context of progressive collapse is defined as the member whose removal causes the most severe damage. Xu and Ye [15] modified the Member Discrete Element Method (MDEM) and perfected it for three aspects: the algorithm itself, loading and computational efficiency, and to accurately and quantitatively simulate the progressive collapse for large-span spatial steel structures.

Nayak et al. [16] studied domes with and without opening. Openings provided at bottom of the dome allow to provide more open area than that at crown which are used for light and ventilation. Tian et al. [17] conducted progressive collapse tests on a scaled single-layer latticed Kiewitt-6 (K6) dome subjected to non-uniform snow load. The failure mode, dynamic response, and collapse mechanism of the tested dome were examined. Zhang et al. [18] investigated the bidirectional and tridirectional isolation systems of large-scale single-layer lattice domes for improving the structural seismic performance and structural vibration control technology. Lee et al. [19] investigated the wind pressure characteristics of an elliptical plan retractable dome roof. Nair et al. [20] investigated the effects of higher modes of multistorey substructures on the seismic response of dome gridshell roofs using response spectrum analysis. Qi et al. [21] studied blast-resistant design considerations for dome structures. The authors investigated the effect of blast load variability on the design value and the structural dynamic response. Fan et al. [22] investigated the applicability of the seismic provisions of the current codes for the nonstructural components (roofing panels and purlins) of single-layer spherical reticulated domes. Zhang and Zhao [23] assessed the seismic resilience of incomplete single-layer reticulated domes and indicated the most unfavorable construction stage, a new curve of recovery functionality and methodology of seismic resilience during construction were established in this study.

Despite a numerous existing theories and structural analysis methods, the structural behavior of domes remains quite uncertain. Domes, mainly Schwedler, lack of adaptable and complete investigation and analysis methods effectively explain the capability of domes. In the present study, the seismic behavior of two types of Schwedler domes with different geometrical parameters has been investigated to explore their efficiency in resisting the earthquake ground motions.

2. Modelling Details

Single layer reticulated (domes composed of bars [24]) Schwedler domes with two patterns of configuration A = Monoclinal Schwedler dome (Figure 2.1) and B = Bidirectional Schwedler dome (Figure 2.2), with 60 m span, having different rise-to-span ratios (h/s=10%,20%,30%), number of meridional ribs (Nn = 8, 12, 24) which are corresponding to plane angles of (45°, 30°, 15°) respectively, number of circumferential rings (Nr = 4, 8, 12). Steel rectangular hollow sections with rigid connections have been used for all structural members, each node has six degrees of freedom, which can translate along the x, y, z directions and rotate around the x, y, z axes. Although the dome is curved in appearance, but all members are straight members.

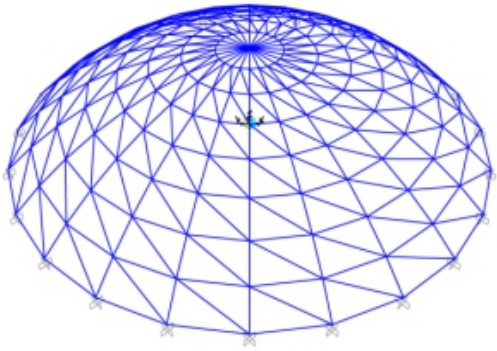

Figure 2.1 Monoclinal Schwedler dome

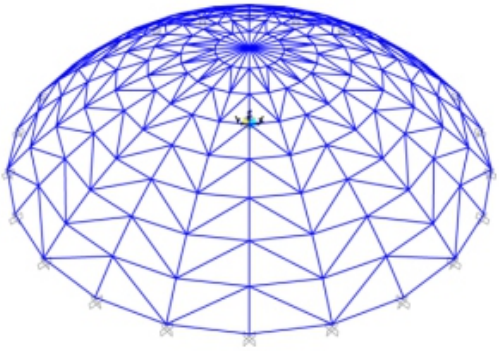

Figure 2.2 Bidirectional Schwedler dome

The simulation of the complex geometry of the space structure was done by using AutoCAD and SAP2000 Version 24 softwares. Two material properties were defined; one for structural members was steel ASTM A36 (Table 2.2) and the other for toughened glass panels (Table 2.3). Table 2.1 summarizes the different parameters of the models. Based on these parameters 54 dome models have been created, Figure 2.3 illustrates the label of analyzed models.

Table 2.1 Analysis parameters of Schwedler reticulated domes.

Parameter of Schwedler domes	Values of the parameter
Span (s)	60 m
Rise-to-span ratio (h/s)	10%, 20%, 30%
Rise	(6, 12, 18) m
Pattern of configuration (A and B)	A = Monoclinal Schwedler dome B = Bidirectional Schwedler dome
Plane angle	(45°, 30°, 15°)
No. of ribs	8, 12, 24
No. of rings	4, 8, 12
Earthquake	El Centro 1940

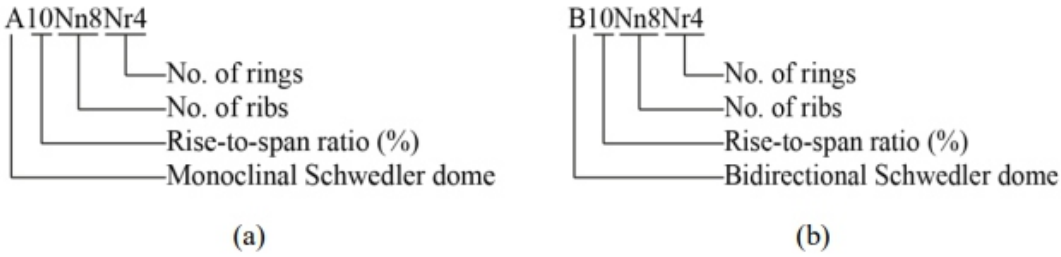

Figure 2.3 Classification of single-layer reticulated Schwedler domes: (a) Monoclinal Schwedler dome (b) Bidirectional Schwedler dome.

2.1 Loading

2.1.1 Dead Loads

The dead load for the dome structure is primarily the own weight of structural members and the cladding. The structural members have been made of rectangular hollow sections. This type of cross section has been chosen because of its insensitivity to the lateral-torsion buckling and hence it is usually used in structures with glass covers [25]. The material used for structural members is steel ASTM A36, its mechanical properties are summarized in Table 2.2.

Table 2.2 Steel ASTM A36 properties.

Yield tensile strength	250 MPa
Ultimate tensile strength	400 MPa
Young's modulus of elasticity	200 GPa
Material density	7850 kg/m^3
Poisson's Ratio	0.3

The glass panels were considered as thin concrete shell elements to simulate the limited lateral restraints to the hoops and ribs members [26]. Table 2.3 illustrates the mechanical properties of toughened glass panels.

Table 2.3 Material properties for toughened glass panels [27].

Modulus of elasticity	70×10^3 N/mm2
Compressive strength (Fcu)	1000 N/mm2
Tensile strength	120 N/mm2
Material Density	25 kN/m3
Linear coefficient of thermal expansion	8 × 10^{-6}/°C
Poisson's ratio	0.22
Thickness	10 mm

2.1.2 Live Loads

The minimum uniformly distributed live load for ordinary flat, pitched and curved roofs is given by ASCE 7-16 to be 0.96 kN/m2[28].

2.1.3 Seismic Loads

Seismic loads arise due to earthquakes. The reason of the seismic load on the structure is acceleration of the supports caused by acceleration of the ground [29]. The most critical seismic load effects can typically be computed using a three sets of ground motions, with two orthogonal components in each set that coincide with the global axes of the 3D model [28]. The three components of El Centro (Figure 2.4),1940, earthquake ground motion are input into the structure in three directions as seismic load. The details of this earthquake are illustrated in Table 2.4.

Table 2.4 Details of the Imperial Valley earthquake ground motion at El Centro Array 9 station [30].

Earthquake Name	Year	Station Name	Magnitude, M_w	Peak ground acceleration, PGA (g)		
				(X-dir)	(Y-dir)	(Z-dir)
Imperial Valley-02	1940	El Centro Array 9	6.95	0.28	0.21	0.18

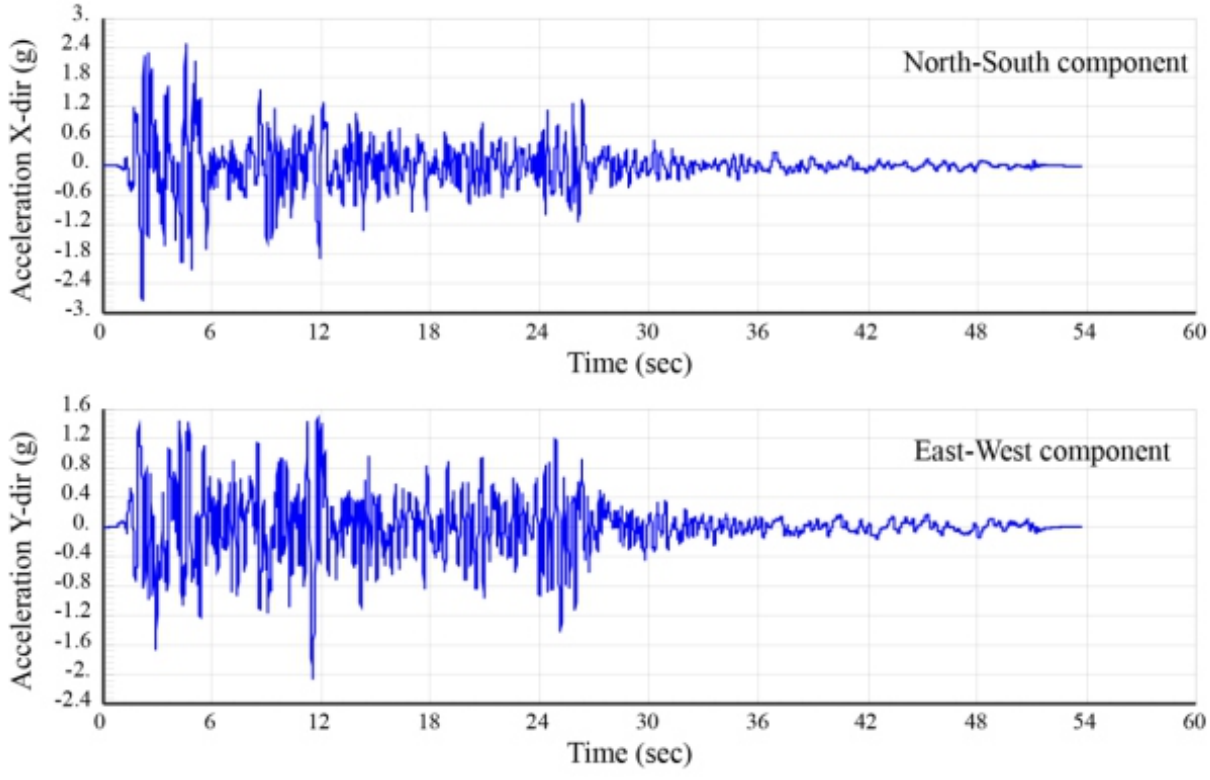

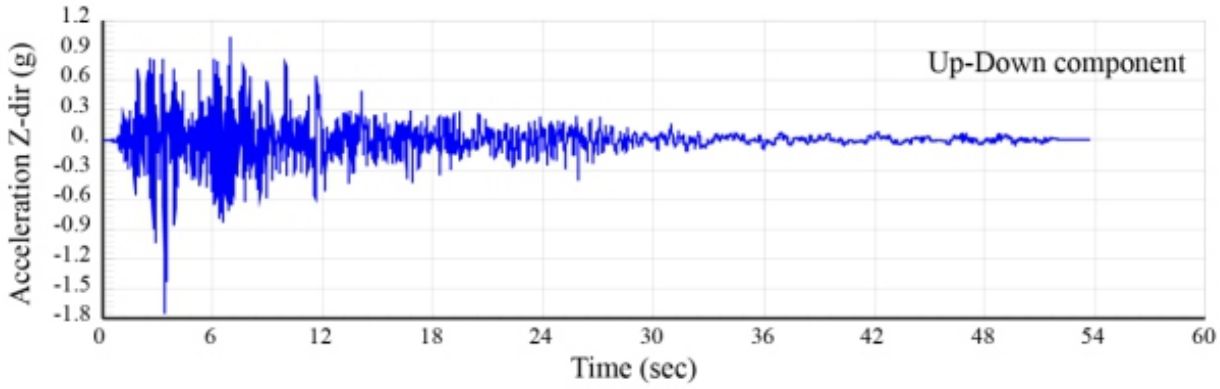

Figure 2.4 North–south and East–west components of horizontal ground accelerations and up down component of vertical ground accelerations recorded at the El Centro Array 9 station, California, during the Imperial Valley earthquake of May 19, 1940.

3. Results and Discussion

3.1 Natural Frequency

As is well-known, free vibration frequency is one of the most important properties of the steel reticulated domes, and it influences the dynamic response of structures under earthquake actions. Therefore, the natural vibration frequencies are supposed to be studied first.Figure 3.1 shows that the natural frequencies of Schwedler domes with 8 and 12 redial ribs and 4 latitudinal rings have frequencies larger than 90 cyc/sec, which have full response in x, y, and z direction with mass participation ratio of 90%, while the other models with natural frequencies less than 30 cyc/sec do not reach 90% of the mass participation ratio in any direction.

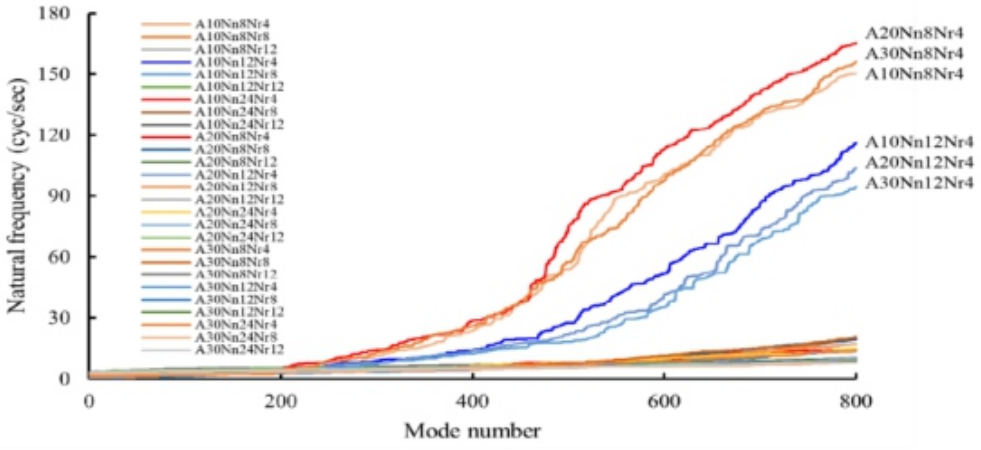

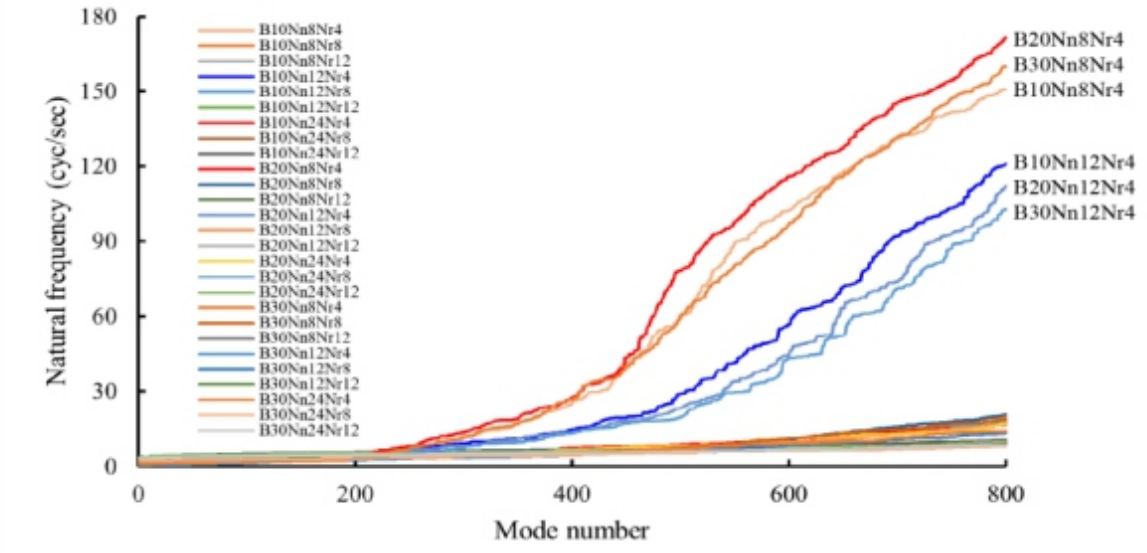

Figure 3.1 Natural frequencies of Schwedler domes with varying parameters.

3.2 Nodal Displacement

Structural displacement is one of the most important dynamic demands for the domes. Numerical results of maximum relative nodal displacement for 54 dome models, 27 models for each pattern of configuration of Schwedler domes, are presented in Table 3.1. These results are obtained by a dynamic linear time history analysis under three-directional seismic loading (El Centro, 1940).

Table 3.1 Maximum relative displacemente in x,y, and z directions.

	Monoclinal Schwedler dome (A-dome)				Bidirectional Schwedler dome (B-dome)			
Model No.	Model	UX (mm)	UY (mm)	UZ (mm)	Model	UX (mm)	UY (mm)	UZ (mm)
1	A10Nn8Nr4	0.62	0.49	3.96	B10Nn8Nr4	0.79	0.63	3.79
2	A10Nn8Nr8	0.82	0.60	4.75	B10Nn8Nr8	0.83	0.60	4.98
3	A10Nn8Nr12	0.79	0.75	8.91	B10Nn8Nr12	0.80	0.70	8.69
4	A10Nn12Nr4	0.69	0.75	3.45	B10Nn12Nr4	0.90	0.92	3.84
5	A10Nn12Nr8	0.68	0.56	4.21	B10Nn12Nr8	0.80	0.60	4.28
6	A10Nn12Nr12	0.75	0.63	6.84	B10Nn12Nr12	0.82	0.70	7.55
7	A10Nn24Nr4	1.77	1.55	5.04	B10Nn24Nr4	1.33	1.17	4.06
8	A10Nn24Nr8	1.27	1.22	5.57	B10Nn24Nr8	1.26	1.08	4.22
9	A10Nn24Nr12	1.24	1.29	7.13	B10Nn24Nr12	1.40	1.28	6.10
10	A20Nn8Nr4	0.92	0.78	2.86	B20Nn8Nr4	1.22	0.80	2.28

11	A20Nn8Nr8	1.44	0.78	4.09	B20Nn8Nr8	1.63	0.98	3.08
12	A20Nn8Nr12	0.80	0.65	3.45	B20Nn8Nr12	0.67	0.52	3.30
13	A20Nn12Nr4	1.57	1.16	2.46	B20Nn12Nr4	1.51	1.32	3.15
14	A20Nn12Nr8	1.20	0.92	3.57	B20Nn12Nr8	1.23	1.00	3.53
15	A20Nn12Nr12	0.83	0.67	2.18	B20Nn12Nr12	0.95	0.78	2.85
16	A20Nn24Nr4	2.47	1.46	3.00	B20Nn24Nr4	2.03	1.34	2.52
17	A20Nn24Nr8	1.75	1.30	4.99	B20Nn24Nr8	2.19	1.42	3.45
18	A20Nn24Nr12	1.34	1.07	3.07	B20Nn24Nr12	1.66	1.58	2.65
19	A30Nn8Nr4	1.84	1.08	2.49	B30Nn8Nr4	1.57	1.04	2.33
20	A30Nn8Nr8	2.21	1.60	2.15	B30Nn8Nr8	2.06	1.48	2.65
21	A30Nn8Nr12	2.09	1.19	2.31	B30Nn8Nr12	2.08	1.25	2.69
22	A30Nn12Nr4	2.59	1.98	2.28	B30Nn12Nr4	2.68	2.00	3.71
23	A30Nn12Nr8	2.17	1.32	2.02	B30Nn12Nr8	1.88	1.28	2.70
24	A30Nn12Nr12	2.18	1.23	2.26	B30Nn12Nr12	2.24	1.14	1.96
25	A30Nn24Nr4	2.63	1.89	2.23	B30Nn24Nr4	2.89	2.05	1.88
26	A30Nn24Nr8	2.86	1.86	1.67	B30Nn24Nr8	3.36	1.96	2.02
27	A30Nn24Nr12	1.93	1.16	2.53	B30Nn24Nr12	1.67	1.08	1.92

3.3 Effect of Pattern on Dynamic Response

Comparison is made for the two patterns of configuration of Schwedler domes, A-pattern which refers to the Monoclinal Schwedler Dome and B-pattern which refers to the Bidirectional Schwedler Dome, Figure 4.20 shows that the two patterns are approximately behaving in the same manner in their dynamic response. That means that the pattern of configuration does not affect the dynamic properties.

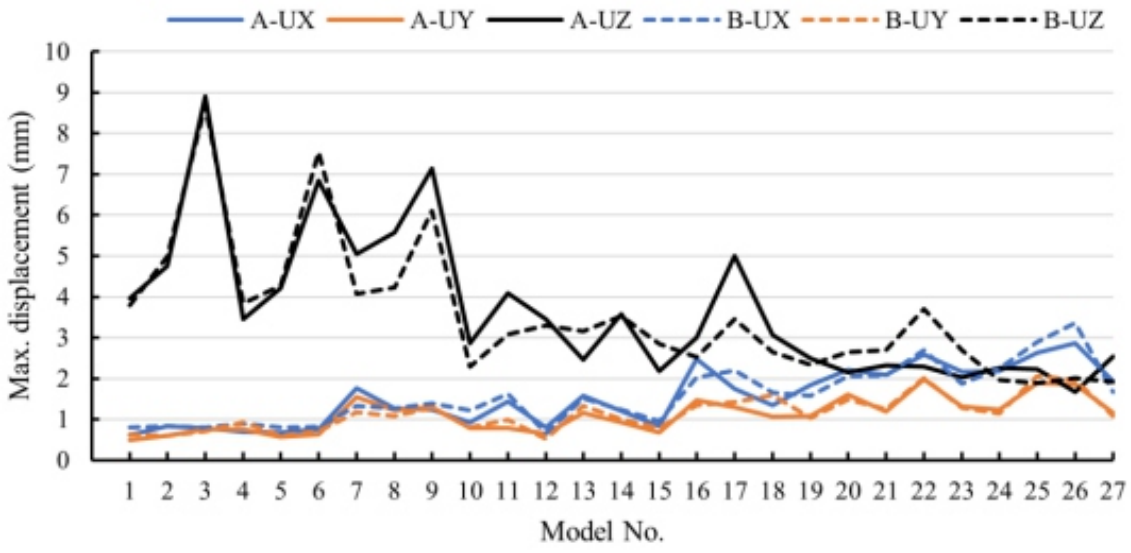

Figure 3.2 Effect of pattern of configuration of A and B models on dynamic displacement.

3.4 Effect of Rise-to-span Ratio on Dynamic Response

As a single-layer reticulated dome under seismic loading is sensitive to the change in shape, the rise-to-span ratio is a key factor having its influence on the shape of the structure. The rise-to-span ratio has also an important effect on the mechanical properties of the structure. It can be clearly seen from Figure 4 for monoclinal Schwedler dome and Figure 5 for bidirectional Schwedler that displacement is significantly enhanced with the decreasing rise-to-span ratio, because the structure with a smaller rise-to-span ratio is flatter and so, the effect of horizontal seismic component is relatively reduced while the effect of vertical seismic component is increased. Consequently, the maximum nodal displacement of both reticulated Schwedler domes increases with the decreasing rise-to-span ratio, because the vertical vibration is the main vibration mode. The rise-to-span ratio of 30% is the most suitable ratio for height of Schwedler domes with 60m span among the three ratios (10%, 20%, and 30%) Figure 3.3.

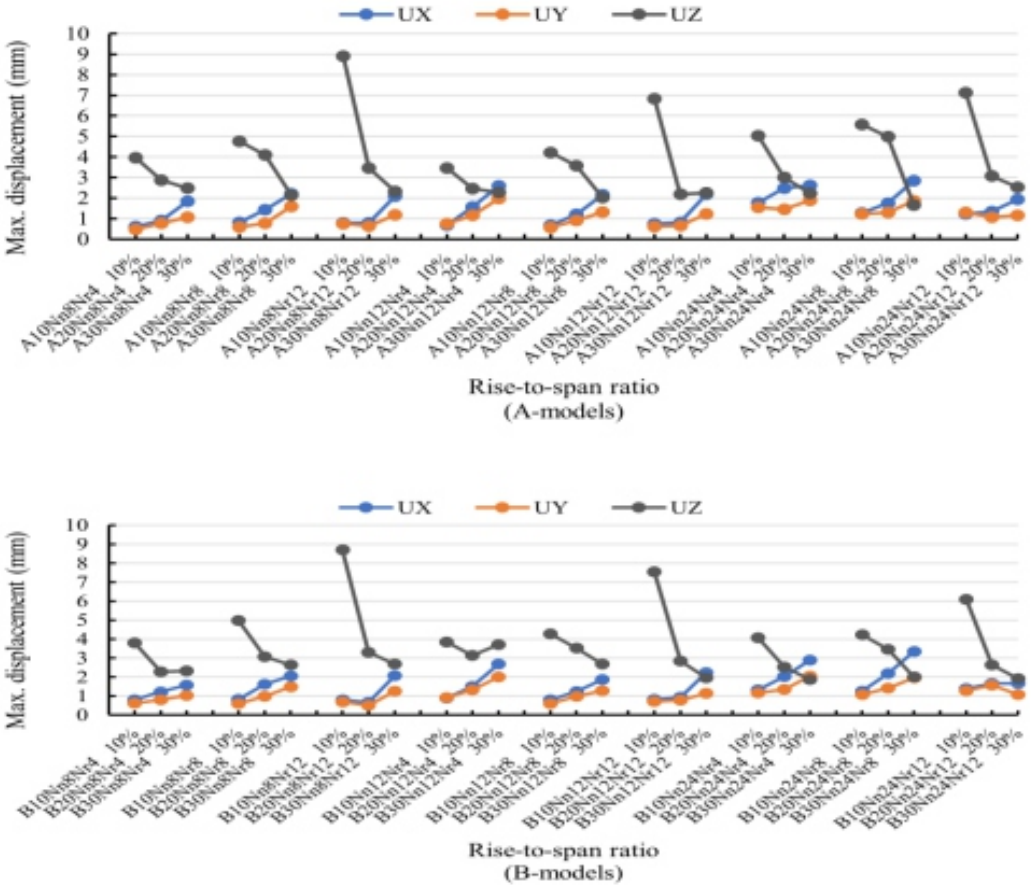

Figure 3.3 Maximum nodal displacement vs. rise-to-span ratio.

3.5 Effect of Number of Ribs on Dynamic Response

Three types of number of ribs (Nn = 8, 12, 24) corresponding to plane angles of (45, 30, 15), respectively, are considered in this study. The effect of Nn on max displacement of Schwedler domes is shown in Figures 4.60 and 4.61.

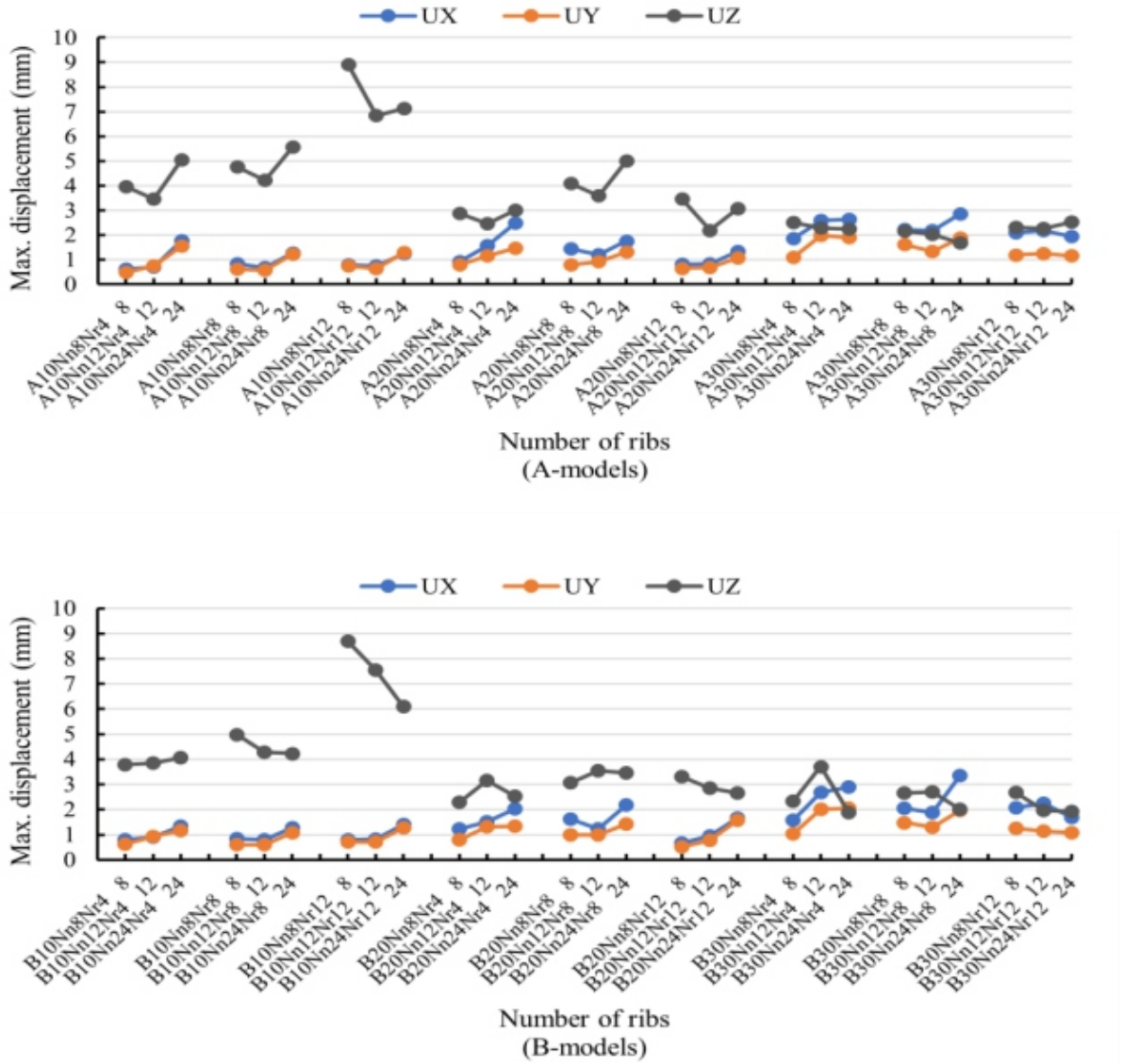

Figure 3.4 Maximum nodal displacement vs. number of ribs (Nn).

3.6 Effect of Number of Rings on Dynamic Response

The effect of increasing the number of rings on dynamic response is shown in Figures

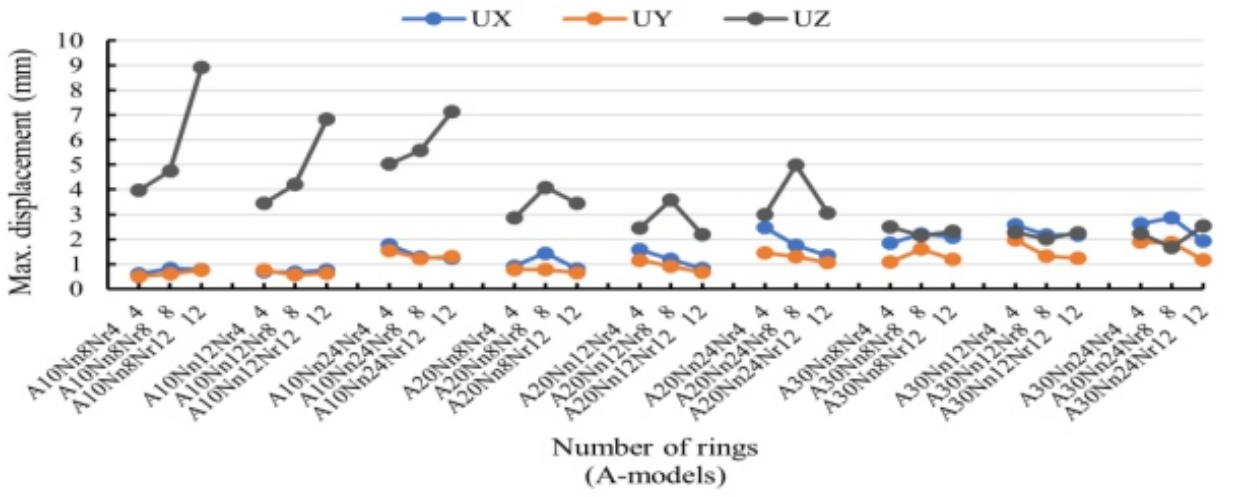

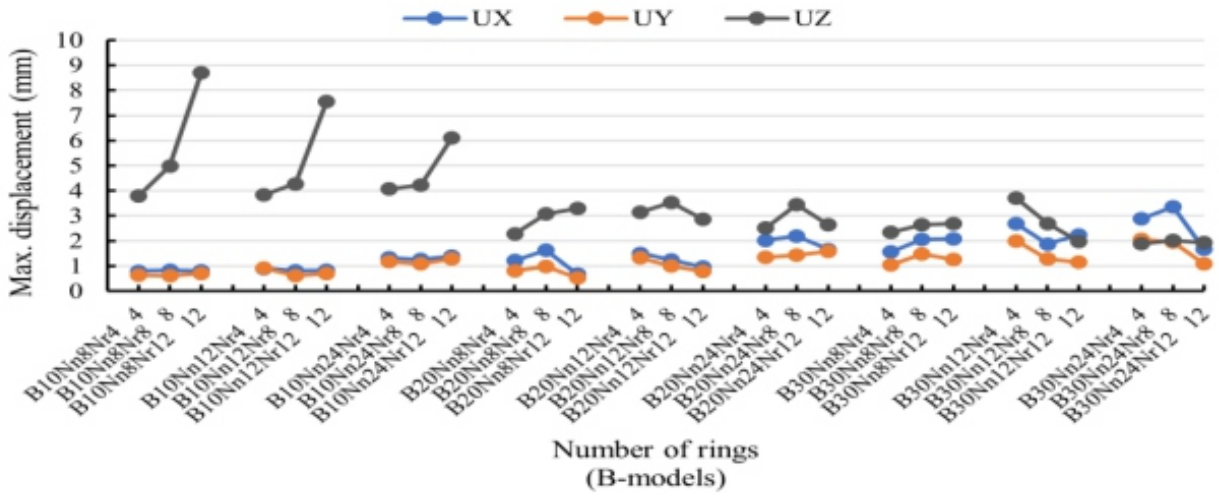

Figure 3.5 Maximum nodal displacement vs. number of rings (Nr).

4. Conclusions

Based on analyses results of single layer reticulated Schwedler dome models subjected to three-directional earthquake ground motion, the following conclusions and recommendations are drawn.

1. The pattern of configuration does not affect the dynamic properties.

2. The rise-to-span ratio of 30% is the most suitable ratio for height of Schwedler domes with 60m span among the three ratios (10%, 20%, and 30%).

3. Schwedler domes exhibit an outstanding performance in severe earthquakes. Light weight, appropriate geometry, redundancy, and large reserve strength are the key elements in such superior behavior.

4. The first mode is not necessarily dominant, and many higher order modes with close frequencies participate in the response, with many modes required to achieve an effective mass ratio of 90%. This makes it difficult to model the seismic response of lattice domes compared to ordinary multistory structures, which are often dominated by just a single mode.

5. As opposed to ordinary buildings, in Schwedler domes higher mode and vertical modes contribute in dynamic response effectively.

6. The models underwent a marked vertical displacement as they were subjected to three-directional excitation, whereas in ordinary buildings, there occurs no significant vertical displacement under three directional excitation.

References

[1] Z. Peng, "Geodesic Dome Structural Analysis and Design," University of Southern Queensland, 2016.

[2] S. A. Behnejad, GAR Parke, and O. Samavati, Inspiring the Next Generation - Proceedings of the

International Conference on Spatial Structures (IASS2020/21-Surrey7). Spatial Structures Research Centre of the University of Surrey, 2022.

[3] D. Pilarska and T. Maleska, "Numerical Analysis of Steel Geodesic Dome under Seismic Excitations," Materials, vol. 14, no. 16, p. 4493, 2021. [Online]. Available: https://www.mdpi.com/1996-1944/14/16/4493.

[4] Y. Qiu, H. He, C. Xu, and B. San, "Aerodynamic optimization design of single-layer spherical domes using kriging surrogate model," Advances in structural engineering, vol. 24, no. 10, pp. 2105-2118, 2021, doi: 10.1177/1369433221992489.

[5] S. Sote, "Structural Analysis of Dome Structure by STAAD Pro," International Journal for Research in Applied Science and Engineering Technology, vol. 9, no. 4, pp. 1515-1520, 2021/04/30 2021, doi: 10.22214/ijraset.2021.33990.

[6] I. Sabri and Z. Abdulzahra, "Effect of Load Distribution on Dynamic Response of Double Layer Grids Space Steel Frames," 2015.

[7] I. S. Salih, S. K. Faleh, and Z. A. Abdulrasool, "Effect of Type of Connection on Dynamic Response of Double layer Grid Space Frames," 2015.

[8] N. A. Jasim, I. S. Saleh, and S. K. Faleh, "Structural Analysis of Ribbed Domes Using Finite Element Method," International Journal of Civil Engineering Research, vol. 8, no. 2, pp. 113-130, 2017.

[9] I. Saleb and T. A. Muhsen, "Dynamic response of braced domes under earthquake load," International Journal of Scientific and Engineering Research, vol. 9, pp. 29-39, 2018.

[10] Z. Yu, S. Li, D. Lu, C. Lu, and J. Liu, "Failure mechanism of single-layer steel reticular domes with reinforced concrete substructure subjected to severe earthquakes," International Journal of Steel Structures, vol. 16, no. 4, pp. 1083-1094, 2016/12/01 2016, doi: 10.1007/s13296-016-0025-8.

[11] H. Ma, Z. Shan, and F. Fan, "Dynamic behaviour and seismic design method of a single-layer reticulated shell with semi-rigid joints," Thin-Walled Structures, vol. 119, pp. 544-557, 2017/10/01/ 2017, doi: https://doi.org/10.1016/j.tws.2017.07.003.

[12] N. Valibeig, S. Rahravi Poodeh, and A. Rahimi Ariaei, "Structural and Geometric Analysis of Discontinuous Double-Shell Persian Domes in Isfahan and Nain Dome-Building Schools," International Journal of Architectural Heritage, vol. 11, no. 8, pp. 1101-1120, 2017/11/17 2017, doi: 10.1080/15583058.2017.1325540.

[13] A. Kaveh, M. Rezaei, and M. Shiravand, "Optimal design of nonlinear large-scale suspendome using cascade optimization," International Journal of Space Structures, vol. 33, no. 1, pp. 3-18, 2018, doi: 10.1177/0266351117736649.

[14] S. Yan, X. Zhao, K. J. R. Rasmussen, and H. Zhang, "Identification of critical members for progressive collapse analysis of single-layer latticed domes," Engineering Structures, vol. 188, pp. 111-120, 2019/06/01/ 2019, doi: https://doi.org/10.1016/j.engstruct.2019.03.027.

[15] L. Xu and J. Ye, "DEM Algorithm for Progressive Collapse Simulation of Single-Layer Reticulated Domes under Multi-Support Excitation," Journal of Earthquake Engineering, vol. 23, no. 1, pp. 18-45, 2019/01/02 2019, doi: 10.1080/13632469.2017.1309606.

[16] C. B. Nayak, M. A. Jain, and S. B. Walke, "Parametric Study of Dome With and Without Opening," Journal of The Institution of Engineers (India): Series A, vol. 101, no. 3, pp. 463-475, 2020/09/01 2020, doi: 10.1007/s40030-020-00447-3.

[17] L.-m. Tian, J.-x. He, C.-b. Zhang, and R. Bai, "Progressive collapse resistance of single-layer latticed domes subjected to non-uniform snow loads," Journal of Constructional Steel Research, vol. 176, p. 106433, 2021/01/01/ 2021, doi: https://doi.org/10.1016/j.jcsr.2020.106433.

[18] H. Zhang, X. Liu, H. Li, and N. An, "A comparative study on the effectiveness of bidirectional and tridirectional isolation systems used in large-scale single-layer lattice domes during earthquakes," Soil Dynamics and Earthquake Engineering, vol. 141, p. 106488, 2021/02/01/ 2021, doi: https://doi.org/10.1016/j.soildyn.2020.106488.

[19] J. H. Lee, Y. C. Kim, D. J. Cheon, and S. W. Yoon, "Wind pressure characteristics of elliptical retractable dome roofs," Journal of Asian Architecture and Building Engineering, pp. 1-17, 2021, doi: 10.1080/13467581.2021.1941996.

[20] D. Nair, K. Ichihashi, Y. Terazawa, B. Sitler, and T. Takeuchi, "Higher mode effects of multistorey substructures on the seismic response of double-layered steel gridshell domes," Engineering structures, vol. 243, p. 112677, 2021, doi: 10.1016/j.engstruct.2021.112677.

[21] S.-b. Qi, G.-y. Huang, X.-d. Zhi, F. Fan, and R. G. J. Flay, "External blast load factors for dome structures based on reliability," Defence Technology, vol. 18, no. 2, pp. 170-182, 2022/02/01/ 2022, doi: https://doi.org/10.1016/j.dt.2021.01.004.

[22] F. Fan, X. Zhi, and W. Li, "Analysis of the Acceleration Response Spectra of Single-Layer Spherical Reticulated Shell Structures," Applied Sciences, vol. 12, p. 2116, 02/17 2022, doi: https://doi.org/10.3390/app12042116.

[23] T. L. Zhang and J. Y. Zhao, "Seismic Resilience Assessment of a Single-Layer Reticulated Dome During Construction," The Hong Kong Institute of Steel Construction, 2022/08/23 2022.

[24] W. Gythiel, C. Mommeyer, T. Raymaekers, and M. Schevenels, "A Comparative Study of the Structural Performance of Different Types of Reticulated Dome Subjected to Distributed Loads," (in English), Frontiers in Built Environment, Original Research vol. 6, no. 56, 2020-May-22 2020, doi: 10.3389/fbuil.2020.00056.

[25] B. Pokusiński and M. Kamiński, "Lattice domes reliability by the perturbation-based approaches vs. semi-analytical method," Computers & Structures, vol. 221, pp. 179-192, 2019/09/01/ 2019, doi: https://doi.org/10.1016/j.compstruc.2019.05.012.

[26] M. M. Y. Kok Keong Choong and J. Y. R. Liew, Recent Advances in Analysis, Design and

Construction of Shell and Spatial Structures in the Asia-Pacific Region. CRC Press, 2020.

[27] F. Cobb, Structural Engineer's Pocket Book. CRC Press, 2020.

[28] ASCE 7-16, Minimum Design Loads and Associated Criteria for Buildings and Other Structures. American Society of Civil Engineers, 2017.

[29] I. A. Karnovsky and O. Lebed, Advanced Methods of Structural Analysis. Springer International Publishing, 2021.

[30] D. R. Majhi and M. Shrikhande, "Residual life of earthquake damaged structures," Soil Dynamics and Earthquake Engineering, vol. 145, p. 106694, 2021/06/01/ 2021, doi: https://doi.org/10.1016/j.soildyn.2021.106694.

Modeling and analysis of the effective parameters on the heat transfer systems in the combustion chamber of engines with liquid fuel

Ali Heidari
Master of Mechanical Engineering, South Tehran Branch, Islamic Azad University, Tehran, Iran

ABSTRACT

Due to high efficiency and lack of contaminants resulting from cryogenic engines combustion as well as high energy content of these motors they are increasing used for space shuttle engines. So, this clarifies the necessity of more analysis of these fuels besides improving the efficiency of internal combustion engines. Prediction of transport phenomena in liquid rocket engines because of some complexities was impossible to be done, but today it happens via using the simulation software. The present research is an attempt to examine the results of modeling and simulation of flow field and the temperature inside the combustion chamber with liquid fuel applying the combustion models in combination with the turbulence models. The simulation results and turbulence model predicted well the temperature inside the combustion chamber. Also, with regard to the simulation results of the combustion chamber, the effects of change of geometric parameters of the cooling ducts on transfer of the engine thrust chamber with liquid fuel. These geometrical parameters include number and frequency of the cooling channels height, fins thickness and the inner wall of the drift chamber. The results indicate that with decrease of flowing cross section of refrigerants from the channel and reduction of the thickness of the inner wall chamber, the wall temperature will also reduce. As the maximum wall temperature occurs in the throat area, increasing the number of cooling channels has a direct impact on the reduction of the maximum wall temperature, but with increase of the height, the maximum wall temperature will increase.

Keywords: combustion gas flow, cooling channels, modeling and simulation of heat transfer, liquid fuel engine

Introduction

Special efficiency and the absence of emissions from the combustion of hydrogen cryogenic propellant and high energy content of the propellant have created very good prospects for the use of this fuel in spacecraft engines. Main engine of space shuttle is among this type of engine uses this fuel (Gutheil, 2001). Therefore, improving the efficiency of internal combustion engines is one of the main issues for combustion science researchers. So, knowledge of the nature of the flow and combustion inside combustion chamber of internal combustion engines to improve their performance is very important (Dinler & Yucel, 2007).

Most rocket engines are of internal combustion type (Reddy et al., 2011). Prediction of transfer phenomena inside liquid rocket engine due to the complexity of many of the conditions in the combustion chamber have not been possible so far (Masquelet, 2006). In the liquid fuel engine, in order

to protect interior wall of the chamber against hot gases caused from the combustion, one of the propellant after passing through the cooling channel wall, is injected into the combustion chamber. Flows into the combustion chamber is mainly of turbulence flows and for analysis of the flow parameters it is needed for modeling turbulent combustion flows. Prediction of heat transfer characteristics in the drift chamber is very important for designing liquid fuel engine with retrieval cooling highly matters. Reducing the wall temperature of the hot gases at about 50 to 100 ° C caused a two-fold increase of chamber life is important in the space missions industry due to the high cost of production. The necessity to enhance the performance of high-pressure combustion devices in liquid-propellant rockets requires high chamber pressures. In a liquid rocket engine thrust chamber, higher chamber pressures allow a higher specific impulse for the engine to be produced. Liquid fuels and/or oxidizers are usually delivered to combustion chambers as a spray of droplets, which then undergo a sequence of vaporization, mixing, ignition, and combustion processes at pressure levels well above the thermodynamic critical points of the fluid. Near the critical point, reactants properties show liquid-like densities, gas-like diffusivities, and pressure-dependent solubility.

Several studies on analysis of heat transfer in liquid-fueled engine drift chamber have been done. Marchi et al (2004) presented a one-dimensional mathematical model for the non-combustible gas in the drift chamber with retrieval cooling. The model is obtained with coupled equations of gas flow in the chamber, the fluidflow in cooling channels and thermal conductivity of the wall. Numerical study of film and retrieval cooling in the drift chamber was performed by Zhang et al (2007). Exchange of heat and mass transfer between the hot gas stream and a liquid thin film inside the chamber with a two-dimensional non-combustible gas flow model and for fluid flow cooling in the channel, a one-dimensional model is used. A 3D model for the numerical simulation of fluid flow in cooling channel of liquid rocket motor drift chamber is provided by Wang et al (2006). They found approximately 335optimal channels with an acceptable pressure drop in the channel. A 2D mathematical model of combustible gas flow in the nozzle of the liquid fuel engine was presented by Cai et al (2007) and VanOverbeke and Shuen (1989). In this model, rradiations effects of gases and retrieval cooling are not considered. Hence, this study aims to model turbulent combustion flow of liquid fuel combustion chamber with the aid of fluid simulation software and temperature parameters inside the chamber with the existing turbulence model. Combustion chamber of advanced rocket uses a liquid oxidizer which, is injected in higher than the critical temperature and pressure into the combustion chamber. Therefore, the surface tension of drops tends to zero, and the droplets get unstable. Because of that, the distance between the liquid and gas phases disappears, the flow can be considered as a homogeneous phase.

Therefore, the Eulerian method flow formula can be used to model the combustion (Benarous, et al., 2007).A one-dimensional mathematical model has been provided to simulate the gas flow in the chamber, the flow pass through cooling channels and thermal conductivity of the wall which, the effects

of cross-sectional area of flow, friction, heat transfer and chemical reactions and gases radiations into the wall are considered.

In the past the research Mayer and Tamura (1996), Candel et al., (1998), Smith et al., (2002) has concerned the cryogenic propellant combustion under subcritical and transcritical conditions, in particular in the case of liquid oxygen and gaseous hydrogen injected from a single element at various chamber pressures (0.1–7 MPa). Recently, there is a great interest in the development of reusable liquid rocket engines operating with methane and oxygen as propellants. Extensive efforts have been made in experimental works to characterize the dynamics of supercritical fluid injection and mixing Chehroudi et al., (2002), Oschwald and Schik, (1999), Mayer et al., (2003) and Oschwald et al., (2006).

Modeling method:

Figures 1 to 3, illustrate the study engine, type of cryogenics coaxial injector fuel injection, and cooling channel geometry respectively. The used fuel is hydrogen and a type of liquid and liquid oxygen oxidizer and the type of combustion is non-premixed combustion. The fuel injection site is on the central axis of the input current. In the study conditions, oxygen at a pressure of 60 bar and a temperature of 100k, speed 4.35m / s and 298k and hydrogen at temperature 298k and speed 168m / s entered into the combustion chamber. In the present study, water is used as a refrigerant in the channels. The chamber pressure was determined 20bar, and input temperature and fluid mass flow rate of cooling were specified respectively 300k, and 20kg /s and the inner wall was made of copper.

To solve the two-dimensional and axial symmetric flow field, a numerical code is increased with turbulence models was used. In this numerical code, the governing equations were dismissed and were performed via volume control method using the simple algorithm. In the location of the flow input speed, boundary condition is input pace and walls in form of constant temperature at 1200k. At the walls place, non slip boundary condition at the wall using standard wall functions was included. In addition to the above components, the radial velocity and zero gradient for the dependent variables, of the flow were applied as the boundary condition in symmetry axis.

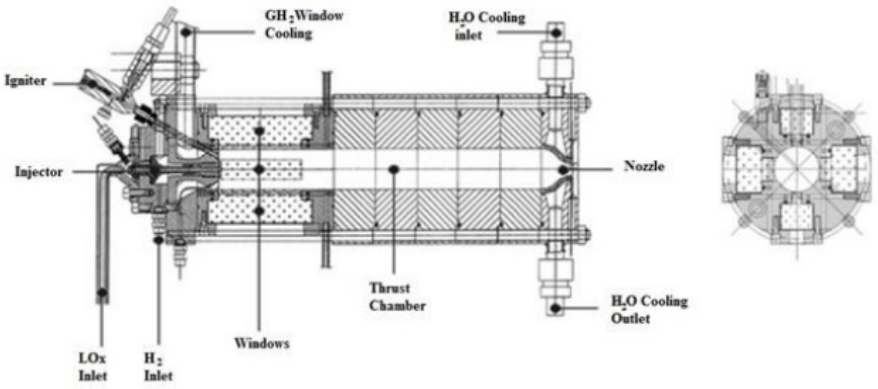

Fig.1: fluid fuel engine with cryogenic (H2-O2)

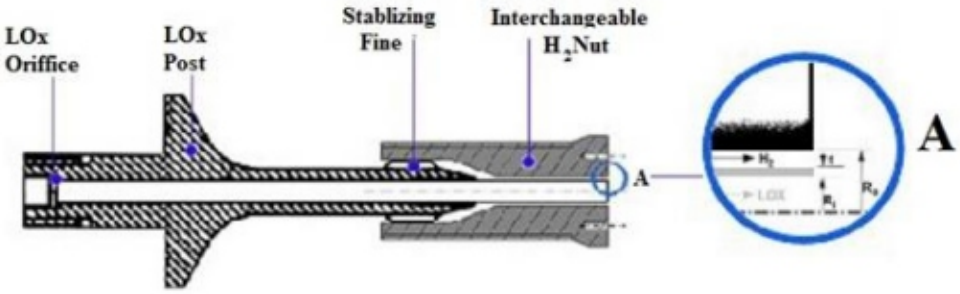

Fig.2: cut in single component with a coaxial geometry change

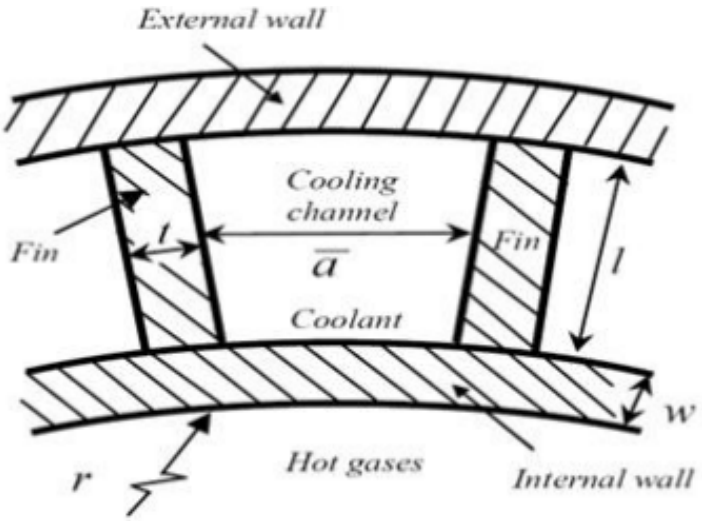

Fig.3: the geometry of cooling channel

Fig. 4 illustrates adiabatic flame temperature close to 3500k which mixing fraction (7.5 to 8.0) temperature of the combustion flame appears. Due to the high difference occurs in fluid mixture it is better to take transitional properties of a varying temperature.

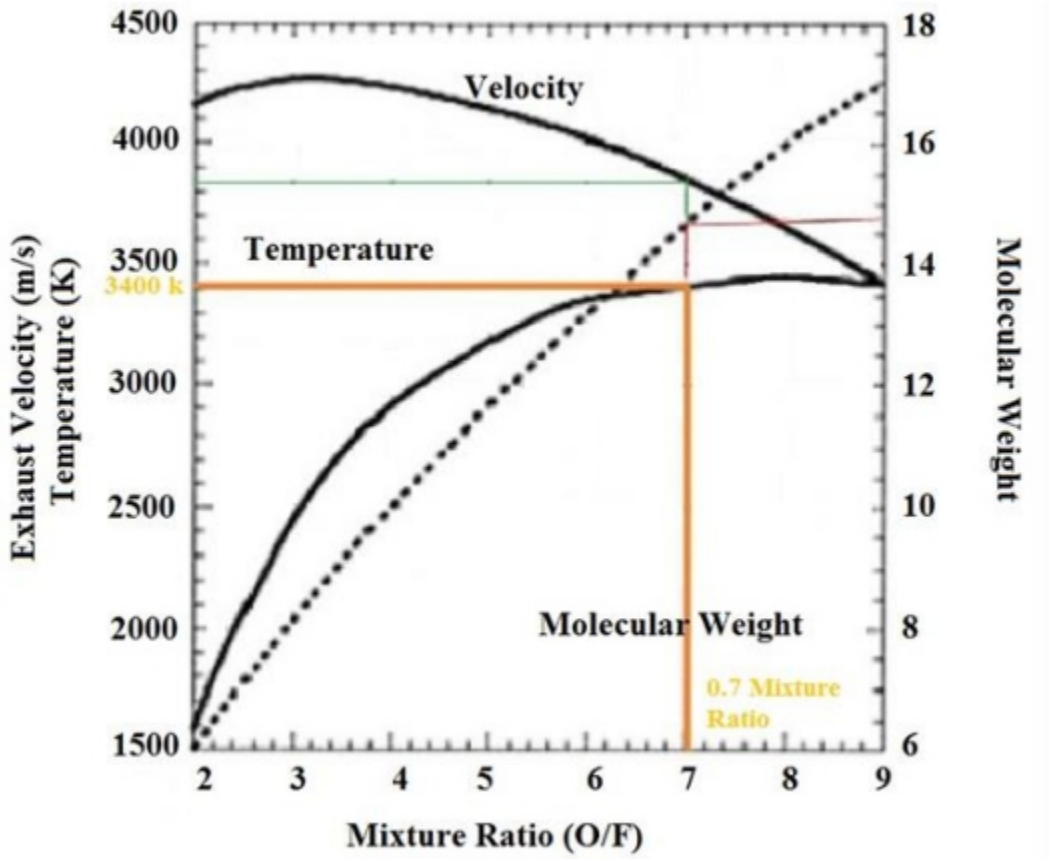

Fig.4: ratio of speed-temperature-molecular weight to mixing fraction of hydrogen-oxygen fuel

$$\lambda(T) = \sum_{i=0}^{4} \alpha_i T^i \quad , \quad \mu(T) = \sum_{i=0}^{3} b_i T^i \qquad (1)$$

Here, viscosity (μ), a & b are constant values, thermal conductivity coefficient (λ) and T is the chamber temperature. For the thermo chemical simulation of combustion a polynomial is adopted only for the gas phase and the method of least squares coefficients a & b and the mixed local density and the mixture law was used for its computation ((Benarous, et al., 2007). In references Takase (1996) and also according to descriptions in Cutrone et al. (2006) and Wilcox (1998), the standard k-1 two-equation model has been used to simulate turbulent heat transfer with Reynolds Averaged Navier–Stokes (RANS) in a limited channel, in the homogeneous phase model, the written in form of Favre average were solved. Chamber inlet turbulent kinetic energy (k) for each flow is as follows:

$k_{f,ox} = 0.00375 U_{f,ox} U^2$

Fuel input rate or oxidizer (Uf,ox), and (u2) is average square velocity. The two-equation model (k-ε) was used with Pop Correction. Using this method, the dynamic behavior of the downstream non-rotating flow of a single injector element is properly expressed.

Table 1: performance conditions of fuel

Performance conditions	H_2	O_2
Pressure	6	6
Temperature	287	100
Mass flux	0.07	0.1
Turbulent kinetic energy	381	178

Combustible the gas flow equations include the mass conservation equation, momentum, energy conservation and molecular components transfer equation where for (NR) preliminary reactions are as follows (Majidi Parsa, 2010).

$$\frac{\partial}{\partial t}(\rho A)+\frac{\partial}{\partial x}(\rho u A)=0 \quad , \quad \frac{\partial}{\partial t}(\rho u A)+\frac{\partial}{\partial x}[(\rho u^2+p)A]=p\frac{dA}{dx}+F' \qquad (3)$$

$$\frac{\partial}{\partial t}(\rho E A)+\frac{\partial}{\partial x}[(\rho u E+up)A]=\frac{\partial}{\partial x}(q_x A)+q' \qquad (4)$$

$$\frac{\partial}{\partial t}(\rho Y_i A)+\frac{\partial}{\partial x}(up Y_i A)=A\dot{\omega}_i-\frac{\partial}{\partial x}(p\tilde{u}_i Y_i A) \qquad (5)$$

$$q_x=\lambda\frac{\partial T}{\partial x}-\rho\sum_{i=1}^{N_s}h_i Y_i\tilde{u}_i \quad , \quad F'=-\frac{\pi}{8}f_g\rho\, u|u|D \, , \quad q'=A'_{wh}\left(q''_h+q''_r\right) \qquad (6)$$

Enthalpy of reaction equation:

$$\frac{\partial\rho h_t}{\partial t}+\frac{\partial\rho u_j h_t}{\partial x_j}=\frac{\partial\rho}{\partial t}+\frac{\partial}{\partial x_j}\left(\rho k\frac{\partial h_t}{\partial x_j}+u_i\tau_{ij}\right)+u_j F_j \qquad h_t=h+u_i u_i/2 \qquad (7)$$

Mass fraction of component equation:

$$\frac{\partial[\rho Y_k]}{\partial t}+\frac{\partial}{\partial x_i}[\rho Y_k u_i]=\frac{\partial}{\partial x_i}\left[\rho D_k\frac{\partial Y_k}{\partial x_i}\right]+\dot{W}_k \qquad (8)$$

Mixed reaction model:

$$R_1=v'^{M_i}A\rho\frac{\varepsilon}{k}\left[\frac{Y_R}{v'_R M_R}\right], \quad R_1=v'_i M_i A.B\rho\frac{\varepsilon}{k}\frac{\sum Y_P}{\sum_1^N v'_j M_j} \quad , \quad \dot{W}_k=Min(R_1,R_2) \qquad (9)$$

Eddy dissipation model:

This model is based on eddy breakdown. The turbulence current is formed from a wide range eddy these eddy consume energy in form of friction and their vanishing process leads to shrinking of the eddy. Finally, they vanish and oxygen and hydrogen enter through separate eddy into the combustion chamber. Eddies are broken and get smaller and are stopped and mixed because of friction.

Turbulence model:

For modeling frictional -eddy current, two equations of standard (k-ε) and (RNG) are used. In this model, two values k and ε are computed via two differential equations. Algebraic stress model, in addition to solving the transport differential equations for k and ε, for obtaining each of the Reynolds stress solves an algebraic equation.

$$\frac{\partial}{\partial t}(\rho k)+\frac{\partial}{\partial x_j}(\rho k u_i)=\frac{\partial}{\partial t}\left[\left(\mu+\frac{\mu_t}{\sigma_k}\right)\frac{\partial k}{\partial x_j}\right]+G_k-\rho\varepsilon \quad (10)$$

$$\frac{\partial}{\partial t}(\rho\varepsilon)+\frac{\partial}{\partial x_j}(\rho\varepsilon u_i)=\frac{\partial}{\partial t}\left[\left(\mu+\frac{\mu_t}{\sigma_\varepsilon}\right)\frac{\partial \varepsilon}{\partial x_j}\right]+C_1\frac{\varepsilon}{k}(G_k)-C_2\rho\frac{\varepsilon^2}{k}-R_\varepsilon$$

$$\mu_t=C_\mu\rho\frac{k^2}{\varepsilon} \quad (11)$$

Here, is thermal conductivity in gases and thermal effects due to the influence of components mass, is frictional drag of chamber, is the effects of heat transfer to wall includes displacement heat flux ,.are modeled as below (Zhang, et al., 2007) and radiant heat flux

$$q_h^{"}=h_g(T_{wh}-T_{aw}) \quad , \quad q_r^{"}=\varepsilon_g\sigma\left(T_{wh}^4-T_g^4\right) \quad (12)$$

Where,

P,u,and Tg are pressure , velocity and temperature of gas, *E* is specific total energy, A is sectional area of flow, *hfi*

is formation enthalpy of component i, is thermal conductivity coefficient of gas, specific enthalpy of component i, is gas density, is infiltration rate of component i, is mass fraction of component *I*, is

Darcy friction factor, D is hydraulic diameter of the chamber, is gas -side wall surface area per unit length x, is coefficient of heat transfer of gas, is gas-side wall temperature, , the Stefan - Boltzmann constant, gas presidents coefficient, adiabatic wall temperature (Zhang, et al., 2007). The subtitles i and Ns show each component and total number of chemical constituents.

To determine the friction coefficient value, the Colebrook equation (Fox & McDonald, 1994) and for determination of the heat transfer coefficient between the gas and the wall, the Bartz equation (Zhang, et al., 2007) were applied. The used chemical model is the combustion air - hydrogen model containing 9 components and 18 preliminary reactions (VanOverbeke and Shuen, 1989). For the preliminary reaction could be written as:

$$\sum_{i=1}^{N_s} v_{ij}' R_i \underset{k_{b_j}}{\overset{k_{f_j}}{\Leftrightarrow}} \sum_{i=1}^{N_s} v_{ij}'' R_i \qquad j=1,\dots,N_R \quad (13)$$

Where,

Ri, Vij and *Vij'* are symbol of component i, the Stoichiometric coefficient of component I irrespectively which are reciprocating in reaction j.

Kfi And *Kbj* are constant rate of reciprocating j reaction which are a function of temperature and gas are determined by the Arrhenius equation.

$$k_{f_j} = A_{f_j} T^{B_{f_j}} e^{-E_{f_j}/\bar{R}T} \quad , \quad k_{b_j} = A_{b_j} T^{B_{b_j}} e^{-E_{b_j}/\bar{R}T} \tag{14}$$

Where,

Free energy of reaction and are energy of releasing sweep j reaction, , , and are constants sweep j reaction. Rate of change of molar concentration of component jth by reaction jth is which concentration of component j is. The overall changing rate of mass concentration of component (ωi) is written as below:

$$(\dot{C}_i)_j = (v''_{ij} - v'_{ij}) \left[k_{f_j} \prod_{l=1}^{N_s} C_l^{v'_{ij}} - k_{b_j} \prod_{l=1}^{N_s} C_l^{v''_{ij}} \right] \quad , \quad \dot{\omega}_i = \sum_{j=1}^{N_R} M_i (\dot{C}_i)_j \tag{15}$$

Specific heat at constant pressure, thermal conductivity and viscosity of each chemical component is determined with a polynomial of degree four (VanOverbeke and Shuen, 1989).The assumption of quasi-one-dimensional flow was used to simulate the fluid passing through thecooling channel.

In this study, cooling fluid with specific mass flow passes from nozzle end through injection channel and flows in opposite direction of passing gas flow in the chamber. The equations consist of continuity equations;momentum size and energy assuming refrigerant density in form of polynomial degree two in terms of fluid temperature are as follows respectively (Marchi, et al., 2004):

$$\frac{d}{ds}(\rho_c u_c A) = 0 \quad , \quad \frac{d}{ds}(\rho_c u_c^2 A) = -A \frac{d\rho_c}{ds} + F' \tag{16}$$

$$c_{pc} \frac{d}{ds}(\rho_c u_c A T_c) = \beta T_c u_c A \frac{d\rho_c}{ds} + q' \quad , \quad \rho_c = \rho + \rho_2 T_c + \rho_3 T_c^2 \tag{17}$$

In these equations, is channel friction drag, includes two works of friction and heat transfer between the walls and is written as below:

$$F' = -\frac{\pi}{8} f_c \rho_c \, u_c |u_c| D \quad , \quad q' = |u_c F'| + A'_{wc} q''_c \quad , q''_c = h_c (T_{wc} - T_c) \tag{18}$$

In the above relation , ‘ ‘ and are used for density, velocity, pressure and temperature of the cooling fluid, S the direction of the flow in channel, A cross-sectional area of the fluid in the channel, specific heat at constant pressure of the cooling fluid, the volumetric thermal expansion coefficient, and and D Darcy friction coefficient and hydraulic diameter of the channel respectively, thermal transfer between the cooling fluid and represents onto the unit of length s, heat flux, heat transfer coefficient between the cooling fluid and the wall and wall temperature of the refrigerant and for solving the equations , the implicit method is extended for combustible flows , were applied for solving the equations for the gas flow.

Simulation results:

In following, the output results of temperature counters in the combustion chamber of engine from the simulation software are presented

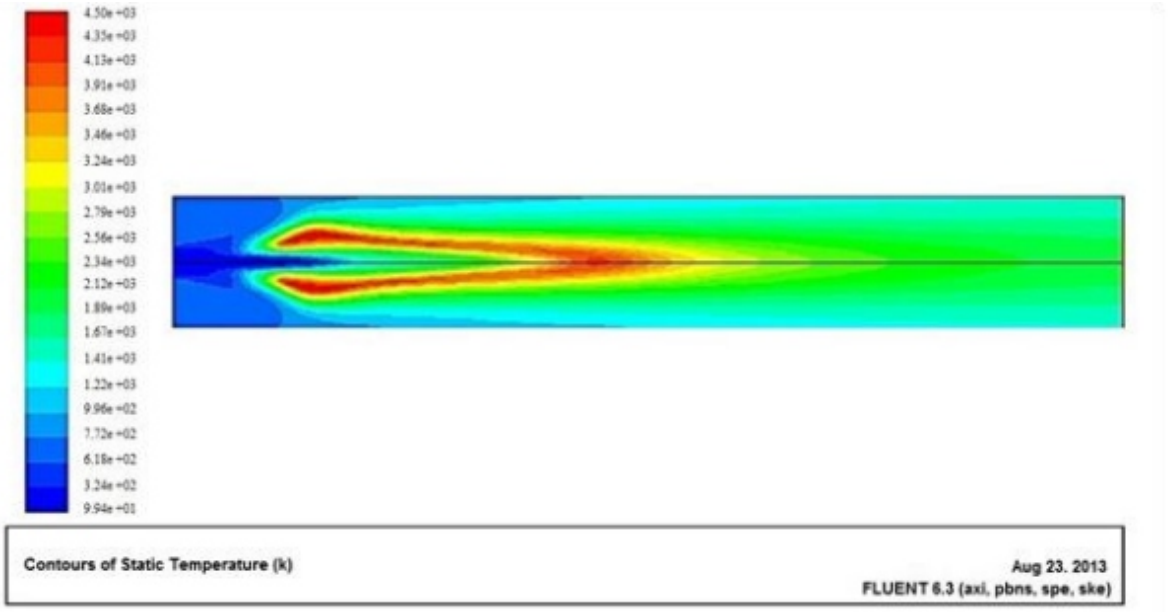

Fig.5: Static temperatures counter in engine combustion chamber

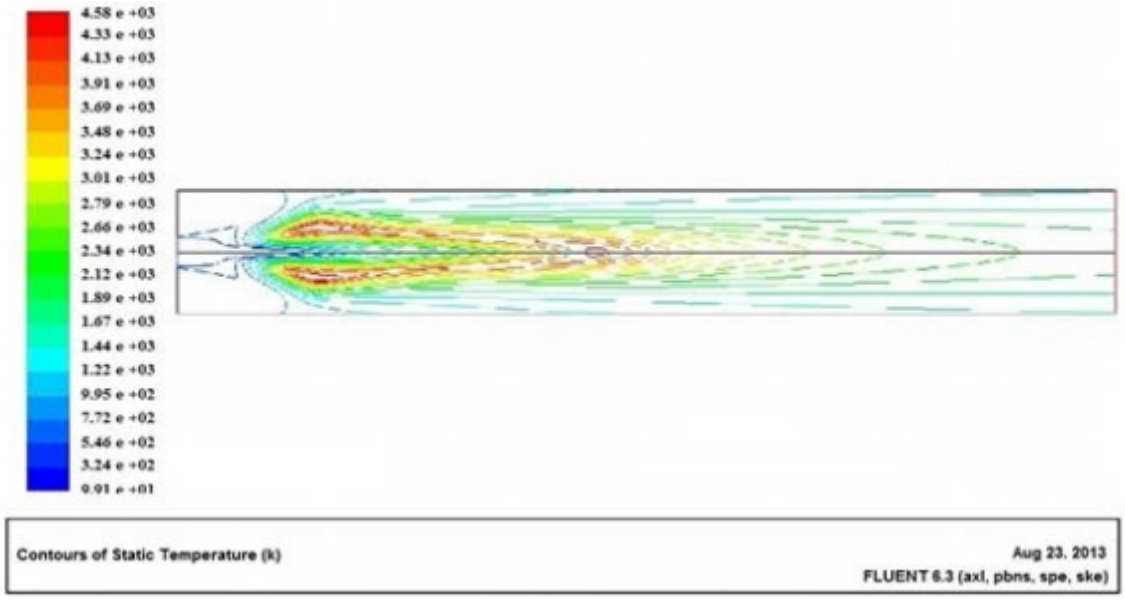

Fig.6: Isothermal contours of static temperature combustion chamber

Combustion temperature in the central part of the screen to the injector changes as: first in the injector inlet to the chamber, since no collision has not lead to sustainable combustion yet, combustion occurs very low and in the boundary layer between two flow directions. The initial temperature is average of

two injected jet temperature into the chamber and approximately 100k. After jet collision and initiation of mixing and combustion, temperature will rise, but the reaction has not reached the required temperature to the highest possible speed. Treatment yet not led to sustained ignition combustion is very low and the boundary layer between the jet stream occurs.

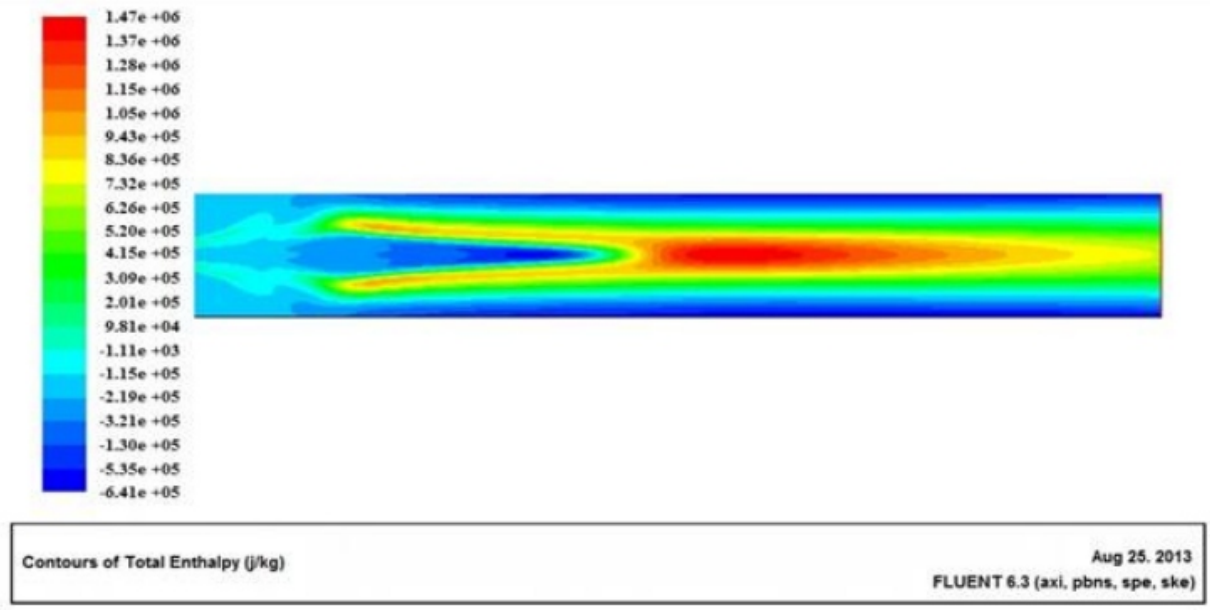

Fig.7: Contour of the reaction enthalpy of combustion chamber

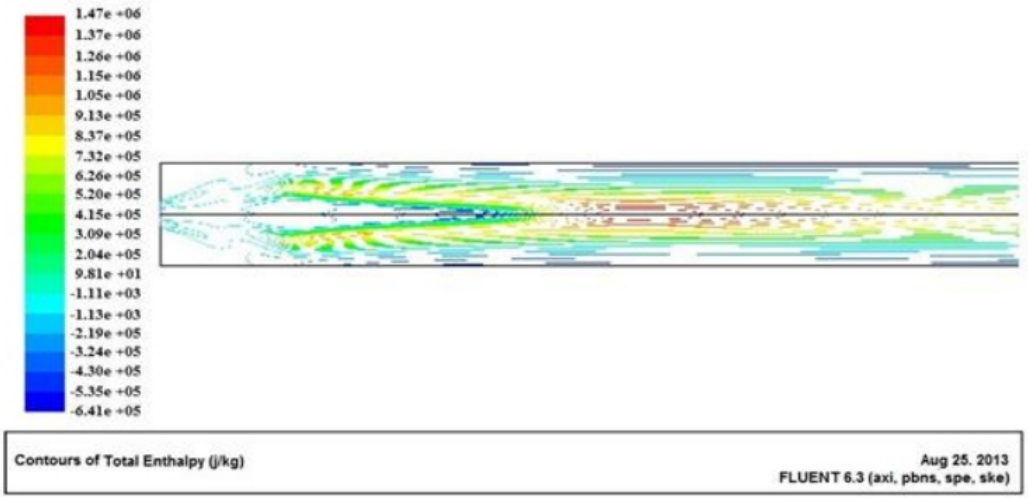

Fig.8: lines with same enthalpy flow over the combustion chamber

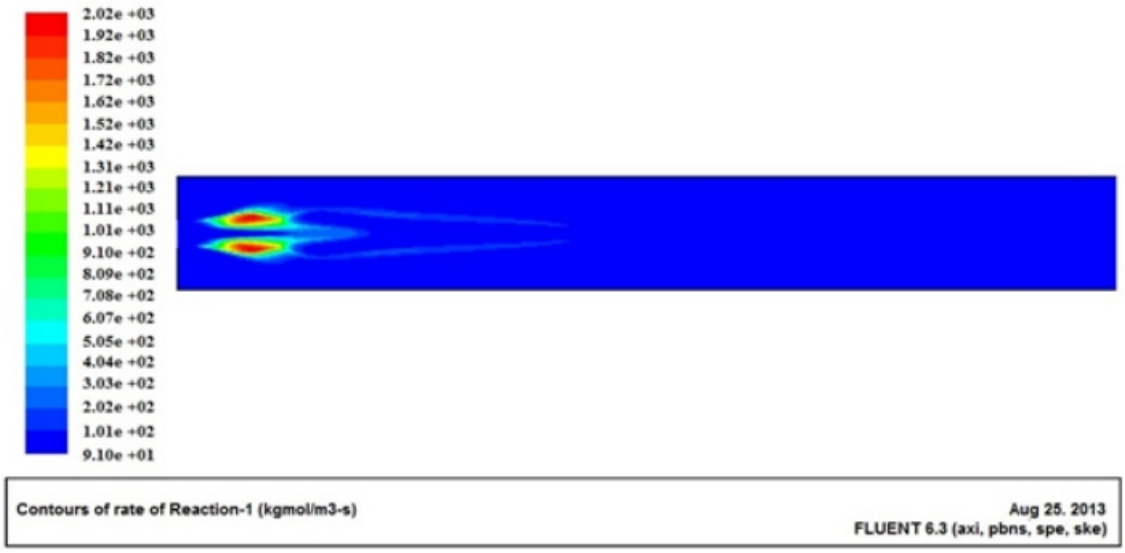

Fig.9: Contour reaction rate turbulent of combustion engine

From 100mm distance the injector goes to completion due to formation of large eddy and temperature increases rapidly due to the formation of hot product again, until it reaches its maximum value over the chamber. After this distance, the reaction reaches equilibrium and the maximum temperature of combustion, mixes with remaining temperature of hydrogen fuel jet with 298k temperature. The temperature begins to decrease and eventually reaches a relatively uniform balance temperature and leads to about 2400k on motor output.

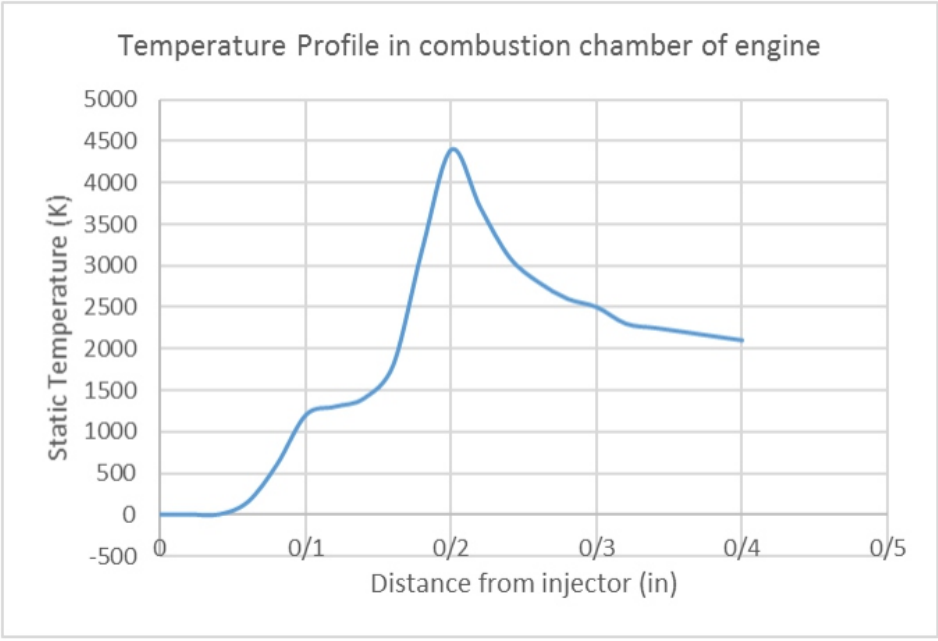

Fig.10: temperature profile in combustion chamber of engine

Comparison of the above and below diagrams indicates that combustion model used in simulation shows properly the temperature of combustion with a difference near 200K. Simulation revealed that

combustion chamber temperature shows a rapid increase in 0.1mm distance and reaches its maximum rate, i.e. 1900K, and combustion gases exit from the chamber with an average temperature of 1900K. As figures 5 and 7 show, the temperature distribution along combustion chamber can be predicted properly by using proper combustion model and the existing method.

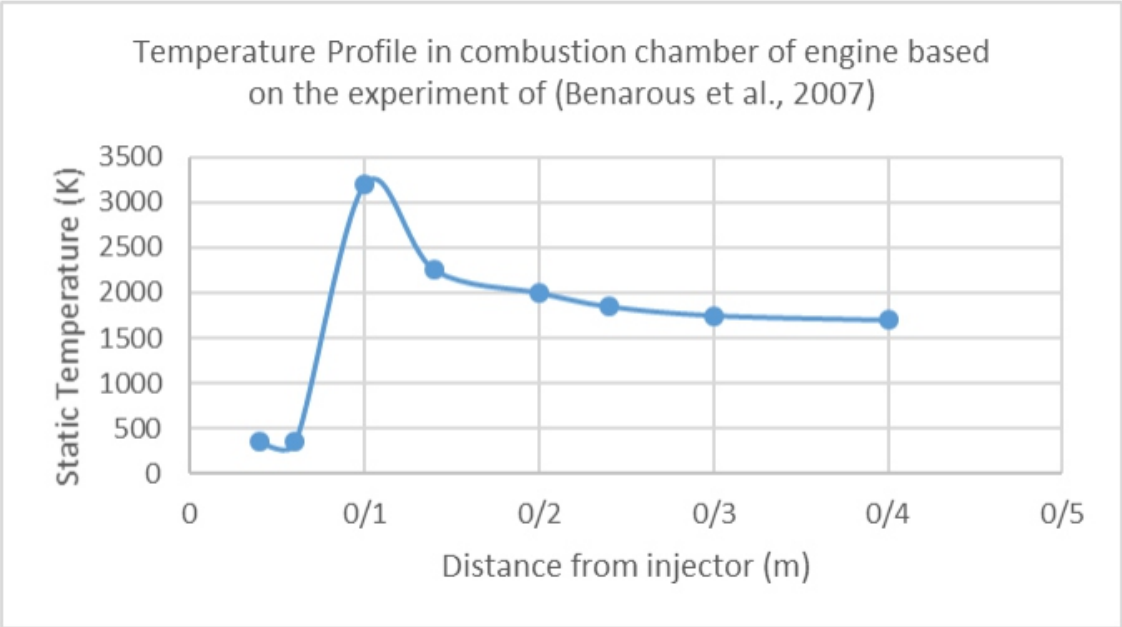

Fig.11: temperature profile in combustion chamber of engine based on the experiment of benarous et al, 2007

The effects of the channel height and the effect of fin thickness and the thickness of the inner wall of the chamber on axial distribution of the wall temperature of the gas-side are shown in Fig.10 & 11.

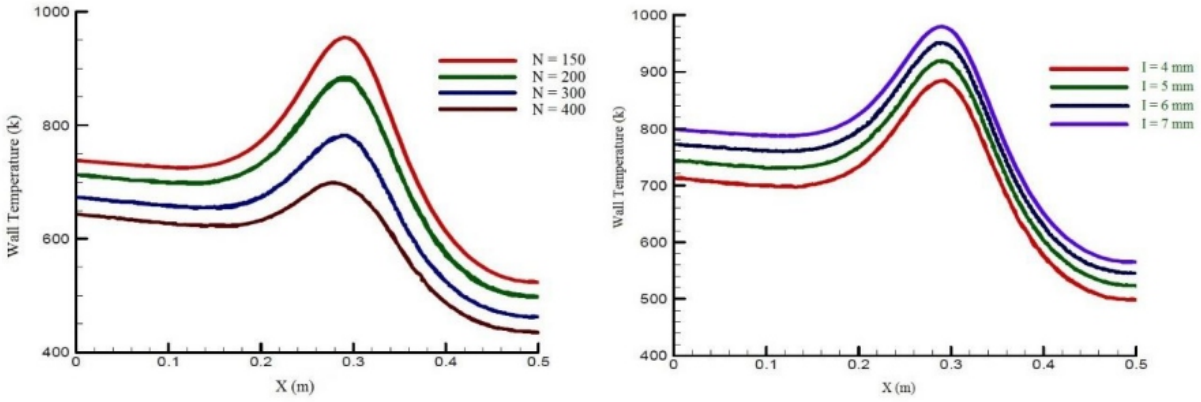

Fig.12: Axial distribution of wall temperature at different number of channels (left) and for different channel height (right)

According to diagram in Fig.10 (right hand side), it could be said that as channel height increases from 4 to 7, the wall temperature rises to about 100 ° K. But increasing number of cooling channels, the wall

temperature reduces about 150 ° K.

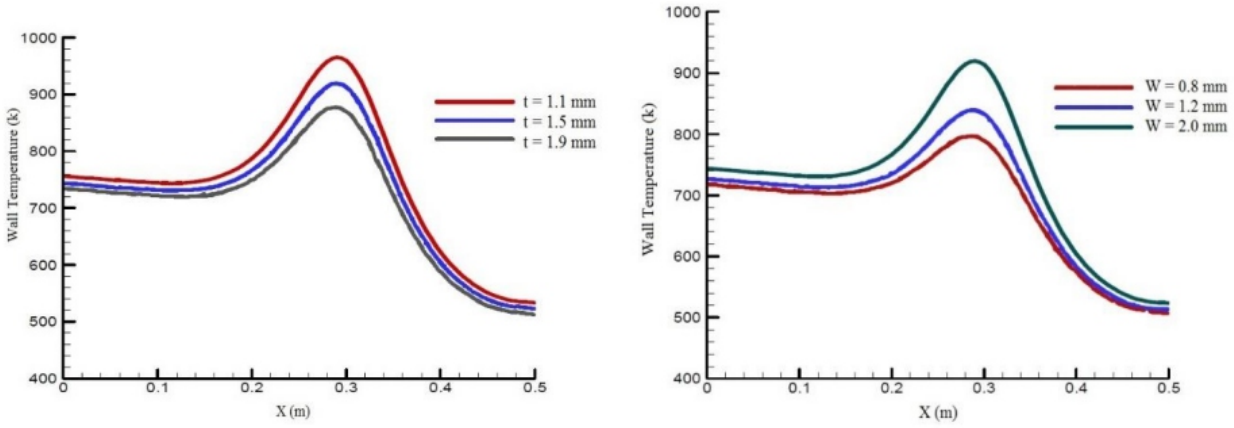

Fig.13: Axial distribution of wall temperature at different thicknesses Finn (left) and different wall thicknesses (right)

Considering the diagram in Fig.11 (right hand side), the right wall temperature will increase withincreasing wall thickness. As the diagram shows, this increase is non-linear and highly progressive. Increase of fin thickness causes reduction in the maximum temperature of the wall. Fig.12 and 13illustrates the effect of changing height and number of channels, Fin thickness and thickness of inner wall on the maximum wall temperature of the gas.

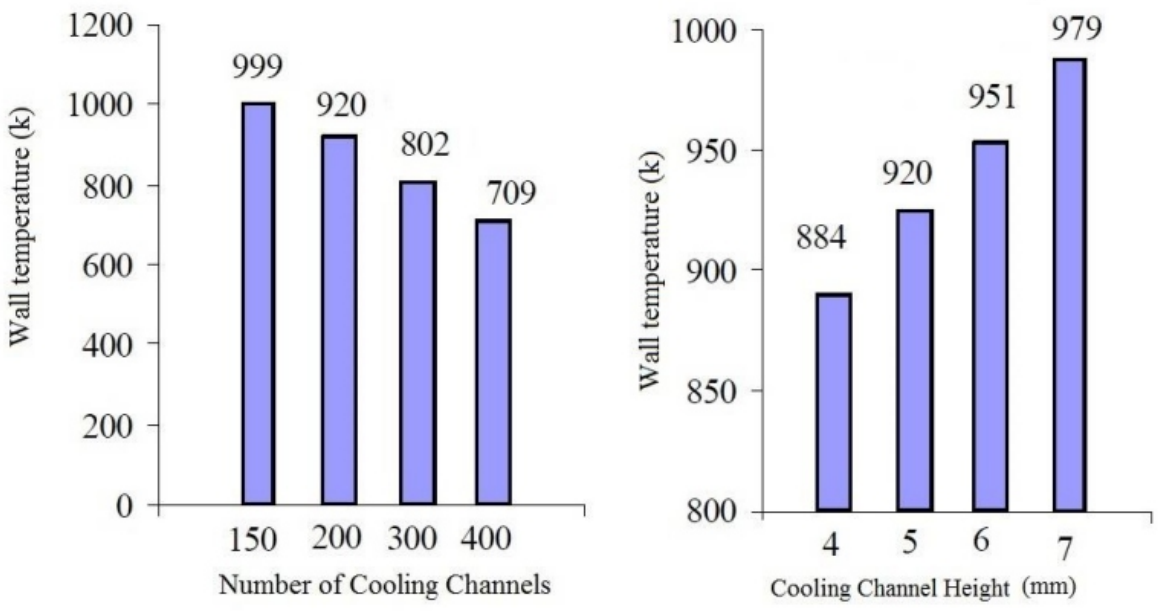

Fig.14: Effect of changes in channel number (left) and channel height (right), the maximum wall temperature

As shown in the above diagram, increasing number of cooling channels has a direct impact on reducing the maximum wall temperature. This reduced temperature is to somewhat close to the curve. About

increase of the cooling channels height it can also be said that with increasing height of the wall temperature will increase due to transfer rules is reasonable and expected.

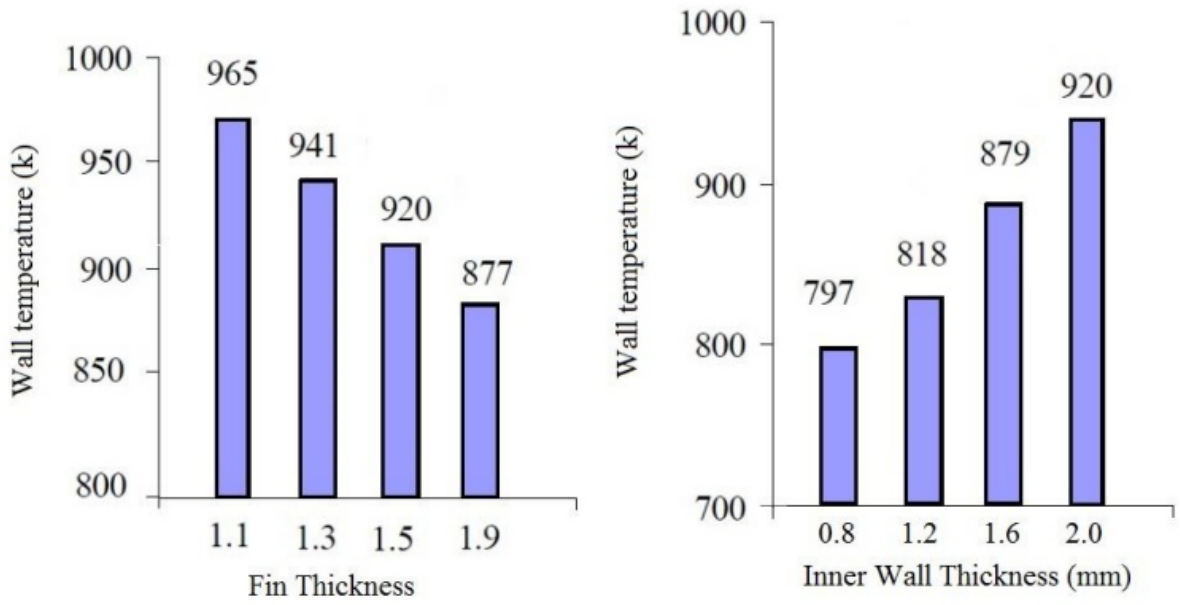

Fig. 15: Evaluation of the effects of fin thickness (left) and the thickness of the inner wall (right), the maximum wall temperature

Diagram 13 shows that with increase of fin thickness, the maximum wall temperature decreases and withincrease of inner wall, as the right hand diagram shows, the maximum temperature will increase which because of the heat transfer characteristics of the wall is reasonably expected.

Conclusion:

The combustion model used in the simulation profile displays well temperature caused by combustionwith a difference approximately 200k. In the injector inlet to the chamber, since no collision occurs yet, no sustainable combustion is created and combustion takes place very low and in the boundary layer between to jets of flows. The initial temperature is an average of two injected jet flows into the chamber and about 100k. After the jets collision and mixing and combustion, temperature shows an increase, but the reaction does not reach h the required temperature for reaching the highest speed. From 100mm distance, the mixing injector goes towards completion due to formation of large eddies and temperature because of formation of a hot product increases rapidly to reach the maximum value over the chamber. After this distance, the reaction reaches equilibrium and the maximum temperature caused by combustion, mixes with the temperature of remaining hydrogen fuel jet at 298k and temperature beans to reduce.

Finally, the effect of geometrical parameters of cooling channels on rate of the rate of heat transfer through the cooling channel wall thrust chamber of liquid-fuel engines, the cooling fluid channel and the thermal conductivity of the walls were studied. For effective cooling thrust chamber,

the wall temperature of the hot gases must be lower than the melting temperature of wall. This can be done by increasing the cooling fluid flow, reduction of cross-sectional area of the fluid passing through the cooling channels by reducing channel height and fin thickness, sex change and reduction of the thickness of the inner wall of the engine.

References:

Benarous, A., Liazid, A., Karmed, D., 2007. "H2O2 Combustion under supercritical Conditions" Third European Combustion Meeting ECM.

Cai, G., Fang, J., Xu, X. and Liu, M., Performance Prediction and Optimization for Liquid Rocket Engine Nozzle, Aerospace Science and Technology, 2007, pp. 155–162.

Candel, S. Herding, G. Scouflaire, P. Rolon, C. Vingert, L. Habiballah, M. Grisch, F. Pealat, M. Bouchardy, P. Stepowsky, D. Cessou, A. Colin, P. 1998. "Experimental investigation of shear coaxial cryogenic jet flames", Journal of Propulsion and Power 14 pp. 826–834.

Chehroudi, Talley, D. and Coy, E. 2002. "Visual characteristics and initial growth rates of round cryogenic jets at subcritical and supercritical pressures," Phys. Fluids 14, pp. 850.

Cutrone, L. Ihme, M. Herrmann, 2006. M. "Modeling of high-pressure mixing and combustion in liquid rocket injectors", Center for Turbulence Research Proceedings of the Summer Program.

Daimon, H. Negishi, H. Kawashima, Conjugated combustion and heat transfer simulations of upper and lower main combustion chambers of LE-9 engine, in: AIAA paper 2019-4112, 2019,

Fox, R.W., and McDonald, A.T., Introduction to Fluid Mechanics, 4th Ed., John Wiley&sons, New York, 1994.

Gutheil, E.; 2001 "Turbulent Spray Combustion Modeling for Rocket Engine Applications" 2nd International Workshop on Rocket Combustion Modeling: Atomization, Combustion and Heat Transfer held in Lampoldshausen, Germany.

Jin Y., Xu X., Yang Q., Zhu S, Numerical investigation of flame appearance and heat flux and in a deep throttling variable thrust rocket engine, Aerosp. Sci. Technol., 88 (2019), pp. 457-467, 10.1016/j.ast.2019.03.042

Leccese G., Bianchi D., Betti B., Lentini D., Nasuti F, Convective and radiative wall heat transfer in liquid rocket thrust chambers, J. Propul. Power, 34 (2) (2018), pp. 318-326, 10.2514/1.B36589

M. Frey, T. Aichner, J. Görgen, B. Ivancic, B. Kniesner, O. Knab, Modeling of rocket combustion devices, in: AIAA paper 2010-4329, 2010, http://dx.doi.org/10.2514/6.2010-4329.

Majdi Parsa, M. (2010). Modeling fluid flow and heat transfer in the thrust combustion chamber of fluid fuel of retrieval cooling, Master's dissertation, Khajeh Nasir Tousi University.

Marchi, C.H., Laroca, F., Da Silva, A.C., Hinckel, J.N., Numerical Solutions of Flows in Rocket Engines with Regenerative Cooling, Numerical Heat Transfer, Vol. 45, 2004. pp. 699–717.

Masquelet M.M., 2006. "Simulations of a Sub-scale Liquid Rocket Engine Transient Heat Transfer in a

Real Gas Environment" Master-thesis, Aerospace Engineering Georgia Institute of Technology.

Mayer, W. Tamura, H. 1996. "Propellant injection in a liquid oxygen/gaseous hydrogen rocket engine", Journal of Propulsion and Power 12 (6) pp. 1137–1147.

Mayer, W. Telaar, R.J. Branam, J. Hussong, J. 2003. "Raman measurements of cryogenic injection at supercritical pressure", Heat and Mass Transfer 39 709–719.

Nureddin Dinler, and Nuri Yucel; 2007 "Numerical Simulation of Flow and Combustion in an Axisymmetric Internal Combustion Engine"world Academy of Science, engineering and Technology, vol. 36.

Oschwald M.and Schik, A. 1999. "Supercritical nitrogen free jet investigated by spontaneous Raman scattering," Exp. Fluids 27, 497, 497–506.

Oschwald, M. Smith, J.J. Branam, R. Hussong, J. Schik, A. Chehroudi, B. Talley, D.2006. "Injection of supercritical fluids into supercritical environment", Combustion Science and Technology 178 (1–3) pp. 49–100.

Reddy, S. K., Pandey K. M., and Singh, A. P., 2011 "Numerical Simulation with K-E Turbulence Model for Combustion Chamber of Rocket Engines" The 11th Asian International Conference on Fluid Machinery and Paper number 220 The 3rd Fluid Power Technology Exhibition, IIT Madras, Chennnai, India.

Smith, J. Klimenko, D. Clauss, W. Mayer, W. 2002. "Supercritical LOX/Hydrogen Rocket Combustion Investigations Using Optical Diagnostics", Paper AIAA-2002-4033, 38th AIAA/ASME/SAE/ASEE Joint Propulsion Conference & Exhibit, Indianapolis.

Song J., Sun B, Coupled numerical simulation of combustion and regenerative cooling in LOX/methane rocket engines, Appl. Therm. Eng., 106 (2016), pp. 762-773, 10.1016/j.applthermaleng.2016.05.130

Takase, K. 1996, "Numerical prediction of augmented turbulent heat transfer in an annular fuel channel with repeated two-dimensional square ribs", Nuclear Engineering and Design, Vol. 165 Nos 1/2, pp. 225-37.

VanOverbeke, T.J., Shuen, J.S, A Numerical Study of Chemically Reacting Flow in Nozzles, AIAA-89-2793, 1989.

Veynante, D., Vervisch, L. 2002 "Turbulent combustion modeling" Progress in Energy and Combustion Science 28 193-266.

Wang, Q., Wu, F., Zeng, M., Luo, L., Sun, J., 2006. "Numerical Simulation and Optimization on Heat Transfer and Fluid Flow in Cooling Channel of Liquid Rocket Engine Thrust Chamber", Numerical Simulation and Optimization, pp. 907-921.

Wilcox, D. C. 1998. Turbulence Models for CFD. DCW Industries, Inc.

Xu J., Jin P., Li R., Wang J., Cai G, Effect of coaxial injector parameters on LOX/methane engines: A numerical analysis, Acta Astronaut., 171 (2020), pp. 225-237, 10.1016/j.actaastro.2020.02.055

Zhang, H.W., He, Y.L., Tao, W.Q., Numerical Study of Film and Regenerative Cooling in a Thrust

Chamber at High Pressure, Numerical Heat Transfer, 2007, pp. 991–1007.

Dual-Axis Solar Tracking Systems for Improved Solar Power Generation Efficiency

Hussain Shaikh1, Kumar Subham2, Diwakar Kumar3, SurveOmkar Millind4, Sanjeet Kumar5, Dr.Harish Harsurkar6,
Department of Mechanical Engineering123456
VPS College of Engineering & Technology, Lonavala, Pune123456

A B S T R A C T

The fluctuation in solar energy happens every day as a result of changes in the day-night cycle and seasonal variations all year long. The world's population is growing at a fast rate. Over the last ten years, non renewable energy sources like coal and oil have been running out, making it difficult to supply the globe with stable energy. Yet a significant source of primary energy is solar energy. This study proposes a dual-axis solar tracking system that makes use of Arduino as the primary processing unit to capture the maximum amount of solar energy.In this study, an autonomous solar tracker system powered by a microcontroller is anticipated to employ photovoltaic conversion panels. Our goal is to create both a single-axis and dual-axis solar tracker system. The tracker follows the sun and adjusts its location to optimise the sun's production of energy. Two geared DC motors are used to move the solar panel in order to maintain the solar panel's alignment with the sun's light.The experimental model's functioning is based on a DC motor that is intelligently controlled by a specialised drive to move a small solar panel. The presence of two cheap but effective light sensors allow a microcontroller to receive data from them. Experimental analysis is done on the solar tracker device's performance and attributes.

Keywords:LDR Sensor, Dual axis solar tracker, Servo motor, Arduino.

1. Introduction

A dual-axis solar tracking system is a type of system designed to increase the efficiency of solar panels by automatically adjusting their orientation to face the sun throughout the day. It uses two axes of movement to track the sun's position in the sky and keep the solar panels aligned with it, maximizing the amount of sunlight they receive[1].

The two axes of movement are horizontal and vertical, with the horizontal axis rotating the panels from east to west and the vertical axis tilting them up and down to follow the changing angle of the sun in the sky. By moving the panels to follow the sun's path, the system can increase the amount of energy they produce by up to 40% compared to fixed, non-tracking systems.

Dual-axis solar tracking systems can be either active or passive. Active systems use motors or actuators to move the panels in real-time, while passive systems rely on changes in temperature or pressure to cause the panels to move. Passive systems are generally simpler and less expensive, but they may not be as accurate as active systems[2]

Overall, dual-axis solar tracking systems are a powerful tool for increasing the efficiency and effectiveness of solar power systems, especially in areas with high levels of solar radiation. They can help to reduce the cost of energy production and make solar power more accessible to a wider range of people and communities.

A solar tracker is a tool that is used to gather solar energy from the sun.Solar tracking is nothing more than shifting a panel's location in relation to the sun. Typically, the photovoltaic module installed in the solar tracker is more powerful than the stationary system's essential irradiance. Based on performance and coast, solar trackers are categorised. By using a tracking system, we may get a 40–50% increase in efficiency over a fixed panel. One of these, dual axis, offers a 48% efficiency boost over single axis tracking. Due to seasonal fluctuations, dual axis trackers can detect the sun's location anywhere in the sky. The solar tracking systems shown in the following images[3].

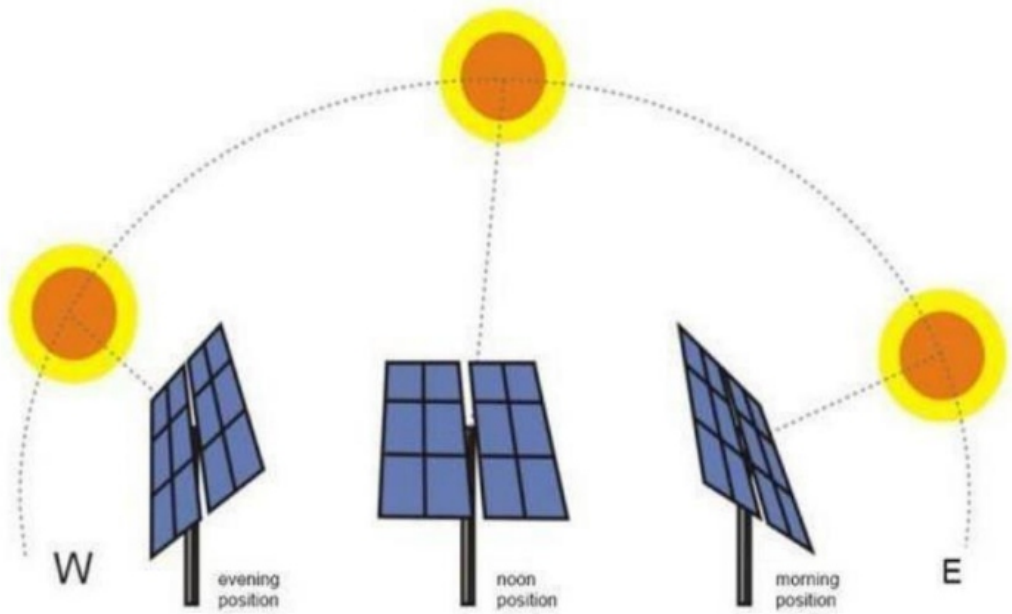

Figure 1. Solar path

2. Literature Survey

Dual-axis solar tracking systems have become an increasingly popular technology for improving the efficiency of solar power generation. As such, there have been numerous research studies and literature reviews on the subject. Here are a few key findings from recent literature surveys:

Efficiency gains: Studies have shown that dual-axis solar tracking systems can improve the efficiency of solar panels by up to 40% compared to fixed, non-tracking systems. This is due to the ability of the system to maintain optimal alignment with the sun's position throughout the day, resulting in increased exposure to sunlight and greater energy production.

Cost-benefit analysis: A literature review conducted by P. J. Sangwaiya et al. (2016) found that while dual-axis solar tracking systems can be more expensive to install than fixed systems, the increased

energy production and resulting cost savings over time can make them a worthwhile investment. The study concluded that the payback period for the additional investment in a dual-axis tracking system is generally less than ten years.

Environmental benefits: Another review by K. S. Reddy and M. K. Tripathy (2018) highlights the environmental benefits of dual-axis solar tracking systems. By increasing the efficiency of solar panels, these systems can reduce the amount of land required for solar power plants and decrease the overall environmental impact of energy production.

Technological developments: Finally, a literature survey by S. S. Patil et al. (2018) emphasizes the importance of ongoing technological development in the field of dual-axis solar tracking systems. Advances in materials science, control systems, and sensor technology are all contributing to the continued evolution of these systems and their ability to maximize energy production from solar panels.Overall, these literature surveys indicate that dual-axis solar tracking systems are a promising technology for improving the efficiency and sustainability of solar power generation. While there are still challenges to be addressed, ongoing research and development in this area are likely to lead to even greater gains in efficiency and cost-effectiveness in the coming years.Haneih's (2009) study highlights the importance of solar tracking systems in increasing the efficiency of PV panels in desert regions. The use of two degrees of freedom orientation and close loop control with solar tracking sensors and feedback control loops can help to optimize the alignment of the panels with the sun's position in the sky, leading to greater energy production.

The consideration of the grid arrangement of panels is also important in maximizing the effectiveness of tracking systems. By carefully arranging the panels in a way that minimizes shading and ensures optimal alignment with the sun, the overall energy output of the system can be further increased.Overall, Haneih's study underscores the importance of solar tracking systems in improving the efficiency and effectiveness of solar power generation in challenging environments like desert regions. By optimizing the alignment of solar panels with the sun's position in the sky, these systems can help to maximize energy production and make solar power more viable and sustainable.

3. Proposed work

The system utilizes LDR (Light Dependent Resistor) sensors to detect any differences in intensity between the sides of the PV panel. If there is a difference, a signal is produced and sent to the control system (circuit1/circuit2) where it is evaluated. The control system then sends a signal to the motor (motor2/motor1) which rotates the PV panel until it directly faces the sun.This system appears to be a type of single-axis solar tracking system, as it only rotates the panel around a single axis to align it with the sun's position in the sky. By using LDR sensors to detect any deviations in intensity, the system can quickly and automatically adjust the position of the panel to maximize energy production.Overall, this type of solar tracking system could be a cost-effective way to improve the efficiency of solar power

generation, particularly in areas with high levels of sunlight. However, as with any technology, there may be limitations and challenges to consider, such as maintenance requirements and the cost of implementing the system on a larger scale.

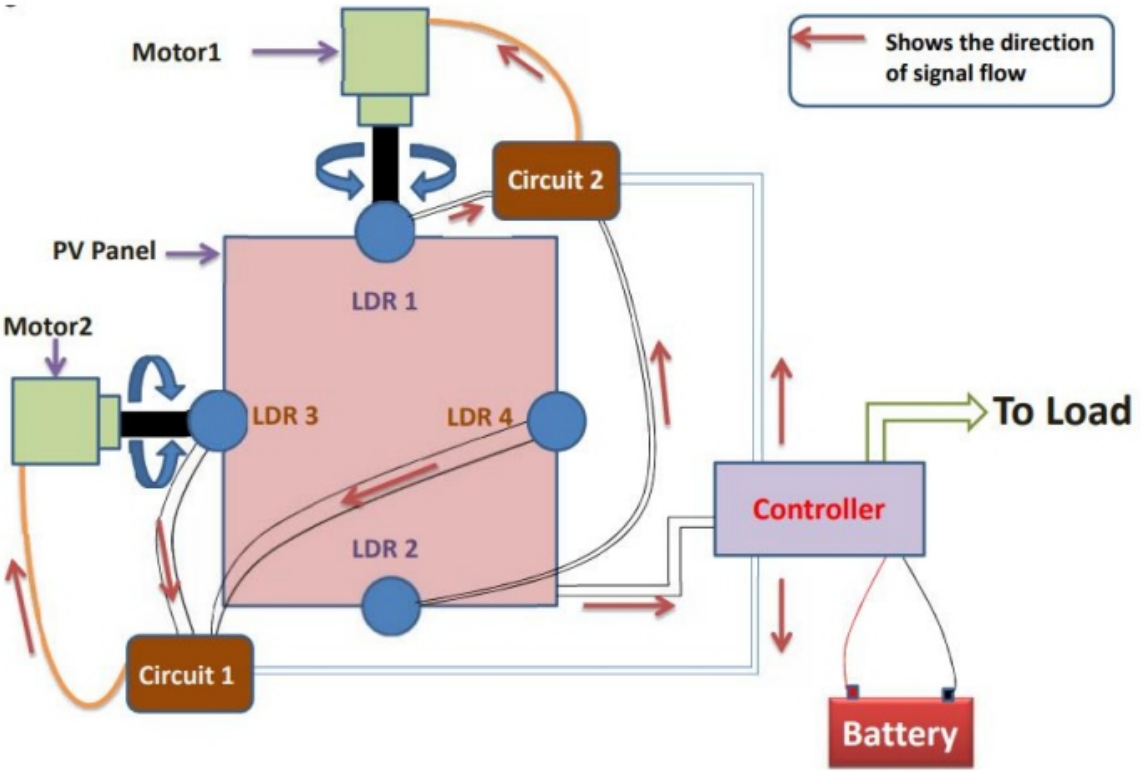

Figure 2: Block diagram of the setup

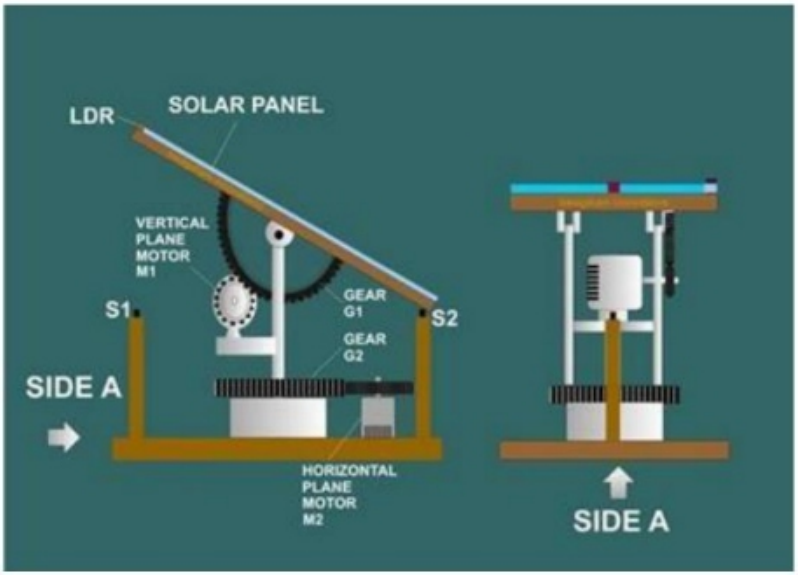

Figure 3. Solar tracking by using sensor, motor and gears

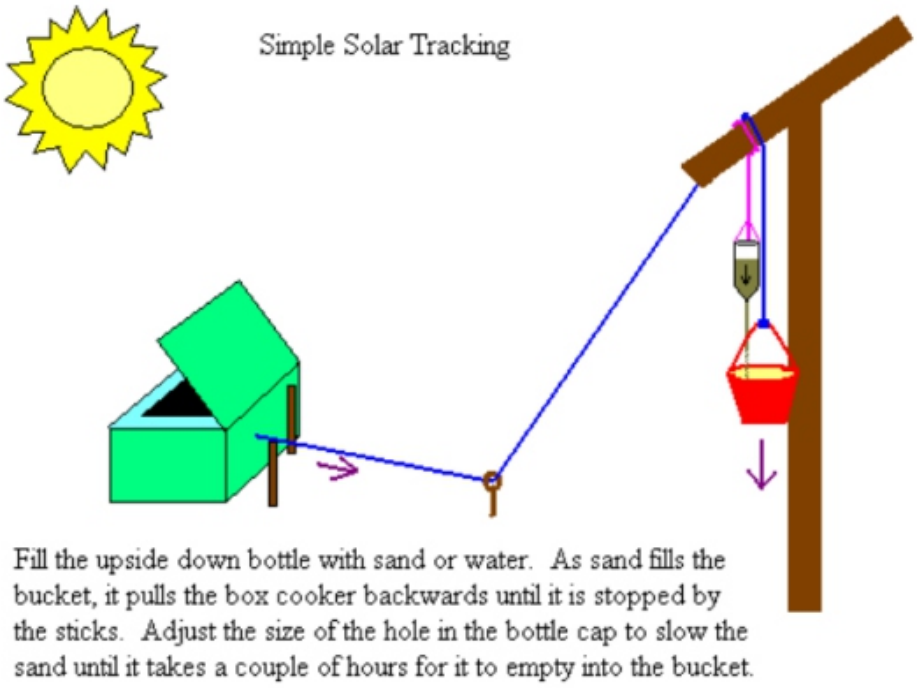

Figure 4. Simple solar tracking by using sand

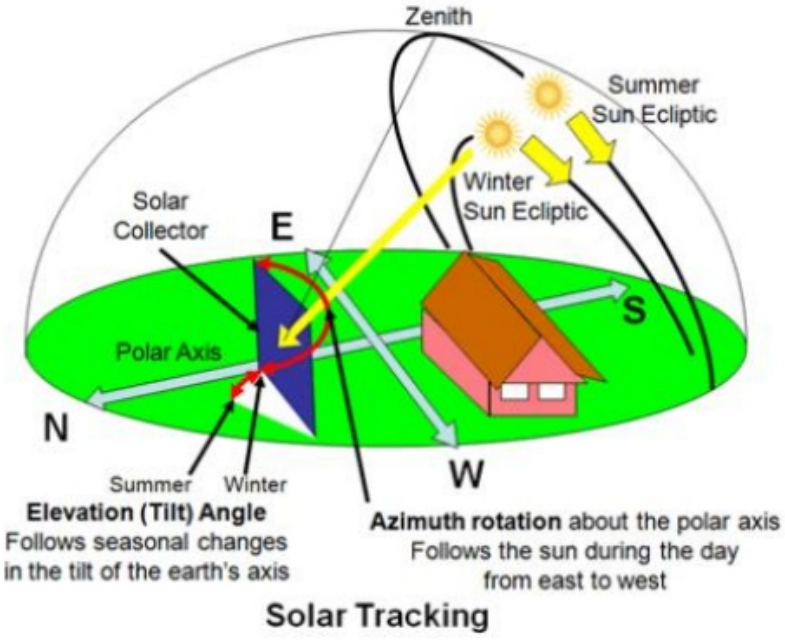

Figure 5. Manual solar tracking

4. Implementation

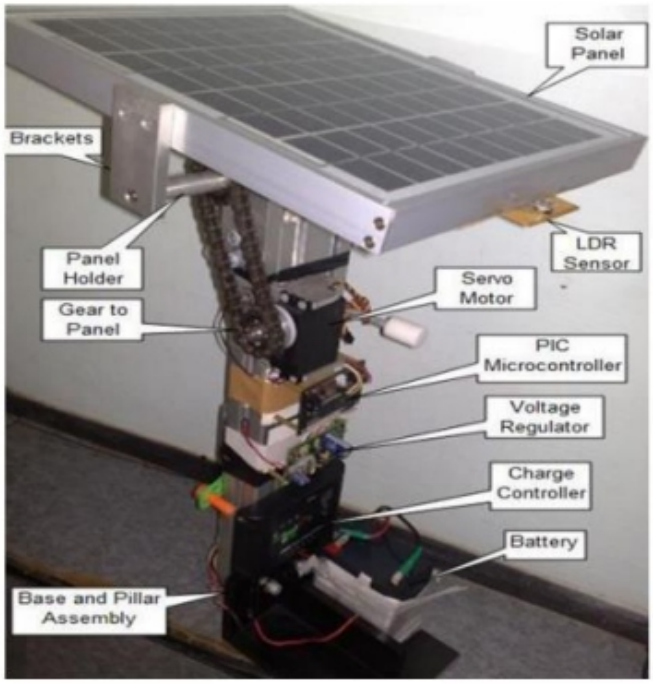

Figure 6. Solar tracking by using chain sprocket and sensors

5. Conclusion

The dual-axis solar tracking system is an effective way to increase the efficiency of solar power generation. By aligning the solar panels with the sun's position in the sky, these systems can maximize energy production and improve the overall performance of solar power plants.Compared to single-axis or fixed solar systems, dual-axis trackers have been shown to provide significantly greater energy output, with studies indicating efficiency gains of up to 40% or more. Additionally, while the initial installation costs of a dual-axis tracker may be higher than other systems, the long-term cost savings resulting from increased energy production can make them a cost-effective investment.

Further research and development in the field of solar tracking systems is likely to lead to even greater efficiency gains and cost savings in the future. Overall, the evidence suggests that dual-axis solar tracking systems are a promising technology for improving the effectiveness and sustainability of solar power generation, particularly in challenging environments like desert regions.

References

[1] Anuraj, A., & Gandhi, R. 2014. Solar tracking system using stepper motor. International Journal of Electronic and ElectricalEngineering, Vol. 7, No. 6, pp. 561–566.

[2] Arsalan, S. 2013. Sun tracking system with microcontroller 8051. International Journal of Scientific & Engineering Research, Vol. 4, No. 6, pp. 2998–3001.

[3] Banerjee, R. 2015. Solar tracking system. International Journal of Scientific and Research

Publications, Vol. 5, No. 3, pp. 1-7.

[4] Deb, G., & Roy, A. B. 2012. Use of solar tracking system for extracting solar energy. International Journal of Computer andElectrical Engineering, Vol. 4, No. 1, pp. 42-46.

[5] Gupta B., Sonkar N., Bhalavi B.S. 2013. Design, construction and effectiveness analysis of hybrid automatic solar tracking systemfor amorphous and crystalline solar cells. American Journal of Engineering Research, Vol. 2, No. 10, pp. 221-228.

[6] Mousazadeh H., Keyhani A., Javadi A., Mobli H., Abrinia K., 2009. A review of principle and sun tracking methods formaximizing solar systems output. Renewable and Sustainable Energy Reviews, Vol. 13, pp. 1800-1818.

[7] Stonecypher L.. 2011. How to Build Your Own Automatic Solar Tracker. Retrieved fromhttp://www.brighthub.com/environment/renewable-energy/articles/76226.aspx

[8] Akhil,K. (March 25, 2016). Solar Tracking System. Retrieved on October 3rd, 2019

[9] Gajadharane, M. R., Gijare, N.A., & Joshi, M. H. (June, 2016). Design and development of mechanical Solar Tracking System. Retrieved on October 7, 2019.

[10] Paul, S., Kumar, D., &Basak, S. (2018). Dual Axis Solar Tracker. Retrieved on 8th October , 2019.

[11] Mishra, J., Thakur, R. & Deep, A. (May, 2017). Arduino based dual axis smart solar tracker. Retrieved on September 29, 2019.

[12] Sreega, R., Nithyananthan, K., & Nandhini, B. (July 02nd, 2017). Design and Development of automated Solar Panel cleaner and cooler. Retrieved on 28 September 2019.

[13] John Connors (2017). Solar Vehicles and Benefits of the Technology. Retrieved on September 25, 2019.

[14] Y.Away and M.Ikhsan, ELSEVIER Automation in construction, (2017), 73, pp. 175- 183.

[15] M.Rumbayan, M.D.Putro, IJESC, 6(11): (November 2017), pp.440-450.

[16] S.Bazyari, R.Keypour, S.Farhangi, A.Ghaedi, K.Bazyari, JPEE, (2014), 2, pp. 718- 728.

ACCELERATION OF E-WASTE GENERATION DUE TO COVID-19 PANDEMIC

Vineet Kumar1, Deepak Kumar Verma2
1 PhD scholar, Department of Civil Engineering, UIET, MDU Rohtak
2 Assistant Professor, Department of Civil Engineering, UIET, MDU Rohtak

ABSTRACT

Beginning in 2020, COVID-19 has been circulating over the globe, and the year 2020 has a projected unmatched mandate for COVID-19 medical supplies and equipment. Out of the medical equipment, work from home, online educations, which depends on technology, accelerates at a high speed. The Social distancing and lockdown meant everything, and everyone turned to technology. To enable their staff to work from home, organizationshastened to install a lot of new equipment. To support distance learning, schools, colleges, universities, and other educational institutions looked for digital platforms and regulations. Families and friends twisted to apps on their smart devices to stay connected to avoid social gatherings. The bulk of the techniques, practices, and technologies used today for managing the forward supply chain of COVID-19 medical equipment, as well as waste produced after use, are wasteful. Work from home and online education practices have increased the use of electronic equipment, resulting in more frequent device breakdowns and an increased burden of E-waste on developing nations rather than developed countries. These unavoidable circumstances and pandemics could create a tidal wave of E-waste in the future. In this review paper, the researcher wants to give a general idea of how E-health and COVID-19 accelerate the generation of E-waste and sustainable development.

Keywords: Covid-19, Pandemic, E-health, Health care instrument, E-waste, and Sustainable development

Introduction

The 2019 corona virus disease epidemic (COVID-19) [2] may go down in history as a watershed point in pandemic history, following the Spanish flu in 1918–1920[1]. In December 2019, this virus first surfaced in Wuhan, China, and within two to three months, it had spread throughout the world. Over 150 million cases and 3 million fatalities worldwide as of May 2, 2021 [3]. Since the corona virus illness of 2019 (COVID-19), which had over 178 million verified cases and killed over 3.86 million people by June 21, 2021, it has spread throughout the world [5],International politeness has been involved with the severe acute respiratory syndrome coronavirus-2 (SARS-CoV-2). The worst-affected nations are those in Southeast Asia, Europe, and the United States. Observers consider how the pandemic may alter how we live, study, and work as COVID-19 spreads over the world.

Through direct physical contact, such as contacting an infected person and touching their eyes, nose, and mouth, as well as respiratory droplets from coughing and sneezing, the coronavirus spreads [5]. Increased reliance on technology that promise to automate and digitize daily life appears inevitable,

even though there are still many unanswered problems [6]. Advances praised in the anthems of the "Fourth Industrial Revolution" include contact tracing apps, virtual workplaces, and classrooms, as well as necessary labor robots [7], the "Zero Marginal Cost Society" or the "Second Machine Age" [8] are in high demand. The proponents of these big narratives readily acknowledge the problems of economic inequality and the impending climatic catastrophe, but their agendas always converge on technological advancement, particularly in robotics, cloud computing, and digital apps [6,7]. The Anthropogenic thesis, which motivates eco-managerial visions of smart cities and sizable, data-driven logistic projects, conveniently fits along with these postindustrial programmes. In discourses on sustainability, "digital solutions" advocate for more and better methods to control the movement of people, things, and information, making the environmental costs of information economies targets for future innovation [9].

By 2020, there will be a big need for COVID-19 medical supplies and equipment. The bulk of the approaches, practices, and technology used today to manage the forward supply chain of COVID-19 medical equipment as well as waste produced after usage are wasteful. All of the following are lacking: traceability, dependability, operational transparency, security, and trustworthiness. They give information on the COVID-19 medical equipment forward supply chain and waste management, and they are also centralized, which could result in a single point of letdown [10].

According to the literature review, the present COVID-19 pandemic [2] has influenced end user electronic device usage patterns and the informal repair and recycle market [11, 12]. Extended use of electronic devices has emerged from work from home, and online education practices [13,14], resulting in frequent equipment failure. The epidemic has had a significant influence on worldwide waste treatment systems. Poor medical waste management could speed the spread of COVID-19, especially in developing countries where waste disposal regulations are less strict [15]. Open landfills are common in the furthermost emerging

Asian countries (Bangladesh, Cambodia, India, Indonesia, Malaysia, Palestine, Philippines, Thailand, and Vietnam), which lack solid waste management [3]. Inadequate garbage disposal practices in developing nations in Africa and elsewhere may result in significant disease outbreaks and environmental concerns [4]. As a result, the goal of this initiative is to encourage proactive planning for the appropriate discarding of COVID-19 waste created in evolving nations. We likewise check to see if there are any links.

Even though a pandemic has long been a plausible scenario and concern, there were insufficient actual measures in place when it struck the world. Furthermore, looking back yielded no assistance. Individual liberty was suddenly threatened by societal well-being. Even essential human factors like nourishment and a social network are no longer selfevident. Every step outside one's door generates concerns about whom one should meet, where one should go, and how close one should go to another human being. The dangerous circumstance brings on stress and unease. Often, the only person one can trust is oneself and common sense. Many people have become reliant on technological gadgets for jobs, schooling, and

relationships. Simultaneously, establishments in many nations have monitored people's lives through their smartphones and other digital devices. Many individuals have been moved by the situation to explore the need for a different path toward a more sustainable lifestyle that uses fewer resources and considers both current and future generations. Education has a crucial role in such a severe circumstance.

E-Health care and E-waste:

E-waste is generated by the electronics goods (laptop, mobile, tablet, printer, and scanner…etc.) and generated by the discarded instruments operated by electricity [16]. Electrical and electronic equipment (EEE) continues to modernise the globe in a number of industries, including business, entertainment, development, and health (sometimes known as E-health due to the usage of Information and Communications Technology (ICT) in the health sector). [17, 18, 19, 20, and 21]. The vast field of ICT application is possibly the world's fastest expanding activity. A substantial surge in creating new electronic items has resulted from extraordinary technological advancement and customer demand. This, along with customers' constant and surprisingly quick switching, has caused a new and extensive problem of dumping vast volumes of 'old' technology, or E-waste. White products, brown goods, and ICT scraps are the three primary kinds of e-waste. According to the literature review, E-health is only one use of ICTs [19, 20]. Though E-health grows in popularity and new technical resolutions are produced, the health and healthcare businesses unknowingly contribute to environmental and human health damage. Diagnostic, monitoring, and laboratory equipment are just a few examples of the types of EEE that have historically been used in the healthcare sector. Possibly the concluding is the greatest concerning of them, especially considering the accompanying transboundary movement worldwide, mostly from developed to underdeveloped nations. Planned obsolescence and "ever greening" of equipment (customer need for the most up-to-date technology) have substantially decreased the usable life of mobile gadgets (Computers (now about three years old) and electronics (about 18 months old), as well as higher turnover and hurriedly increased E-waste capacity [22]. Therefore, the COVID-19 pandemic's impact on e-health has a big impact on how much E-waste is produced in the future.Numerous possible environmental hazards, as well as valuable mechanisms, may be found in e-waste due to the occurrence of toxic materials (e.g., metals like lead, cadmium, and mercury, as well as polymers like polyvinylchloride (PVC) [23]. E-waste has the potential to pollute the air, land, and water, causing harm to the ecosystem. As a result, if E-waste is not correctly handled and disposed of, it poses a risk to human health. To avoid environmental harm and health hazards, E-waste disposal must be managed in an environmentally sound manner [23, 24, and 25].

Telemedicine and E-waste:

Through the COVID-19 pandemic, the importance of telemedicine in health care service delivery became apparent in both poor and industrialized nations [16-17]. Telemedicine's usefulness in battling

the COVID-19 epidemic has also been extensively demonstrated in several other nations, including China, the United States, and Singapore, where telehealth infrastructure is well developed. Furthermore, the rising number of COVID-19 cases has put pressure on most countries' healthcare systems. Patients involved in treating these patients' found trips to hospitals for other problems unappealing since health care workers are at increased risk of COVID 19 infection [15]. During the COVID-19 pandemic, telemedicine was effectively employed to address several services and delivery elements of health care. According to a literature review and studies, it is used in triaging and screening COVID-19 symptoms, contact tracing, COVID-19 symptom monitoring, providing specialized care for COVID-19 patients who are hospitalized, providing mental health services and support to COVID-19 patients, caregivers, and frontline health care workers with psychological issues, and monitoring. During the COVID-19 pandemic, many developed and developing countries adopted telemedicine for better medical treatment. Telemedicine is an ICT-driven field requiring electronic equipment such as computers, cellphones, printers, speakers, laptops, tablets, routers, and cameras. With the adoption of telemedicine in many nations, the demand for these electrical gadgets will undoubtedly rise, as will the development of E waste. This is expected to exacerbate the existing e-waste problem, particularly in underdeveloped nations. There is little question that is relying on telemedicine has significant health risks. Nations, particularly developing countries, must be careful not to bite off more than they can chew in the future by exposing their populations to further health risks while attempting to treat current health issues.

E-Waste and COVID-19:

Agriculture, industry, healthcare (from here on "healthcare"), electronics, municipal waste, radioactive waste, and food wastes are just a few of the wastes produced by human activity [26]. Before the pandemic, E-waste was considered the waste generated domestically and industrially by discarded electronic goods, electrical goods. Medical radioactive, municipal, and electronic wastes, for instance, are or could pose a health danger to people. The most important challenges faced by the urban municipalities and healthcare providers during the COVID-19 pandemic (Ilyas et al., 2020; Manupati et al., 2021) and the following 2–5 years is the disposal of healthcare wastes, particularly thermal guns, pulse oximeters, ventilators, oxygen concentrators, and other electronic goods.

E-waste is the most widespread sort of household garbage all around the world. The World Health Organisation (WHO) reports that 53.6 million tonnes of e-waste were generated globally in 2019, an increase over previous years20. Africa is the world's fourth most populated continent, and it generates a substantial amount of E-waste20. The lack of importation standards meant to check the quality of imported products, the smuggling of commodities across boundaries, and the donation of inferior or outmoded technical equipment are all distinct components that contribute to this burden. Because e-waste contains dangerous substances such as poisonous metals and organic compounds, it must be appropriately managed and disposed of. A direct influence might cause the negative impacts of e-waste

on human health.

Sustainable Development:

Deep considerations of aims and epistemology and carefully selecting methodologies, equipment, and technology are essential in sustainable education. It is all about ethics. Many educators believe that digital learning is the answer to the Covid-19 challenge. Even if many people have become dependant on online learning and working through digital gadgets, no one can claim this is a long-term solution. You may save money and time by using digital tools. They minimize travel (mostly in wealthier countries); nevertheless, they have a darkside and do not promote sustainability under present international law. However, there is a strong possibility that this may widen the difference between winners and losers on a worldwide scale and within pupils. E-waste created by technological devices may be detrimental to one's health and the environment—the E-waste scavengers in countries agree to receive the used E-waste [24,25].Prior to COVID-19, the world already had a significant issue with the management of solid waste, particularly E-waste, and after COVID-19, the production of E-trash increased in developing countries relative to developed countries worldwide. So, on sustainability concern, the developing countries try to develop such infrastructures to reduce the burden of E-waste through proper disposal, dismantling and treating improperly, and training the people involved in these industries.

The scenario of India in Pre and Post COVID-19:

With about 3.23 million metric tonnes of e-waste produced each year, India is now the third-largest producer of e-waste in the world, behind the US and China.Computer equipment makes up more than 70% of India's e-waste, followed by telecom/phones (12%), electrical equipment (8%), and medical equipment (2%), according to a survey of the literature. India is currently in the worst 10 nations out of 180 in the World Economic Forum's 2018 Environmental Performance Index. While almost nothing ends up in a landfill, the informal sector is handling 95% of E-waste, a significant concern source. Between 2018 and 2020, India's e-waste creation increased by about 43%. The COVID-19 epidemic, which increased electronic and electrical equipment usage, is expected to bring this issue to light shortly.According to a literature review, India has been the only country in South Asia since 2011 to have a dedicated legislative framework for dealing with e-waste. This law was passed in India in 2011 and went into force in 2012. The E-waste standards were revised twice more in 2016 and 2018. While the legislation of 2012 required takebacks, they did not set a target or provide incentives—some adjustments made in 2016 increased regulatory clarity by establishing progressive and increasingly tighter collection objectives. The most recent modifications in 2018 increased EPR collection objectives by 10% per year through 2023. Following that, the aim was set at 70% of the total amount of E-waste created.The requirement for ecologically suitable e-waste management, as well as its transportation, storage, and recycling, is covered by the E-waste (Management and Handling) Rules. Additionally, they proposed the

concept of "extended producer responsibility" (EPR). The Producer Responsibility Organisation (PRO) and buy-back, deposit refund, and exchange programmes were added to the statutes in 2016. However, because of high handling and procurement expenses, low margins, and underutilization of capabilities, the majority of E waste handlers in the official sector or recognised by the pollution control board are battling serious problems. The epidemic has an impact on the game as well because more equipment is added as work and schooling go online.

Conclusion

The e-waste catastrophe is not impending; it has already arrived. A developing country's ability to modernize society and technology-dependent enterprises is critical. All through the COVID-19 widespread, the government and the PPP model private sector scrambled to rebuild health facilities. On the contrary hand, laws should be created and strictly enforced by governments to control the standard of imported electronics. The environment should be made favourable for e-waste recycling activities by the government, or at the very least encouraged. This ensures that unstructured actions are well-regulated and environmentally friendly. The general public should be taught about the potential health dangers associated with E-waste and recycling, particularly unmanaged versions. However, social responsibility and healthcare ethics require that we ignore the negative effects of e-health on the environment (including telehealth, e-learning, knowledge translation, storage of health data, cloud computing, and other application extents) and that we instead concentrate our creative energies on finding ways to lessen these effects, particularly the e-waste produced by enabling health and healthcare.. Aside from the health sector, it also made sure that E-waste generated by was recycled and put the right rules and legislation into place to reduce the environmental impact and landfills.

Reference:

[1] Yang, Wan, Elisaveta Petkova, and Jeffrey Shaman. "The 1918 influenza pandemic in N ew Y ork C ity: age-specific timing, mortality, and transmission dynamics." Influenza and other respiratory viruses 8, no. 2 (2014): 177-188.

[2] Goldstein, Joshua R., and Ronald D. Lee. "Demographic perspectives on the mortality of COVID-19 and other epidemics." Proceedings of the National Academy of Sciences 117, no. 36 (2020): 22035-22041.

[3] Dutta, Deblina, Shashi Arya, Sunil Kumar, and Eric Lichtfouse. "Electronic waste pollution and the COVID-19 pandemic." Environmental Chemistry Letters (2021): 1-4.

[4] Sangkham, Sarawut. "Face mask and medical waste disposal during the novel COVID-19 pandemic in Asia." Case Studies in Chemical and Environmental Engineering 2 (2020): 100052.

[5] Galloway, Summer E., Prabasaj Paul, Duncan R. MacCannell, Michael A. Johansson, John T. Brooks, Adam MacNeil, Rachel B. Slayton et al. "Emergence of SARS-CoV-2 b. 1.1. 7 lineage—united

states, december 29, 2020–january 12, 2021." Morbidity and Mortality Weekly Report 70, no. 3 (2021): 95.

[6] Khreiche, Mario. "The cost of labour and energy in digital media and automation technologies beyond the COVID-19 pandemic." Journal of Environmental Media 1, no. 2 (2020): 8-1.

[7] Schwab, Klaus. "The Fourth Industrial Revolution: what it means, how to respond. World Economic Forum." In World Economic Forum. https://www. weforum. org/agenda/2016/01/thefourth-industrial-revolution-what-it-meansand-how-to-respond, Accessed July, vol. 21, p. 2019. 2016.

[8] McAfee, Andrew, and Erik Brynjolfsson. "Human work in the robotic future: Policy for the age of automation." Foreign Affairs 95, no. 4 (2016): 139-150.

[9] Kuntsman, Adi, and Imogen Rattle. "Towards a paradigmatic shift in sustainability studies: a systematic review of peer reviewed literature and future agenda setting to consider environmental (Un) sustainability of digital communication." Environmental Communication 13, no. 5 (2019): 567-581.

[10]Ahmed, Syed Ishtiaque, Steven J. Jackson, and Md Rashidujjaman Rifat. "Learning to fix: knowledge, collaboration and mobile phone repair in Dhaka, Bangladesh." In Proceedings of the Seventh International Conference on Information and Communication Technologies and Development, pp. 1-10. 2015.

[11]Ahmad, Raja Wasim, Khaled Salah, Raja Jayaraman, Ibrar Yaqoob, Mohammed Omar, and Samer Ellahham. "Blockchain-Based Forward Supply Chain and Waste Management for COVID-19 Medical Equipment and Supplies." IEEE Access 9 (2021): 44905-44927.

[12]Jackson, Steven J., Syed Ishtiaque Ahmed, and Md Rashidujjaman Rifat. "Learning, innovation, and sustainability among mobile phone repairers in Dhaka, Bangladesh." In Proceedings of the 2014 conference on Designing interactive systems, pp. 905-914. 2014.

[13]Rifat, Mohammad Rashidujjaman, Hasan Mahmud Prottoy, and Syed Ishtiaque Ahmed. "The breaking hand: Skills, care, and sufferings of the hands of an electronic waste worker in Bangladesh." In Proceedings of the 2019 CHI Conference on Human Factors in Computing Systems, pp. 1-14. 2019.

[14]Chetna Krishna. 2020. Can the pandemic help us to embrace refurbished electronics? https://www.dw.com/en/can-the-pandemic-help-us-to-embracerefurbished-electronics/a 53741181. (Accessed on 10/12/2020).

[15]Kevin Pratt. 2020. Mobile Phone Use Surges During COVID-19 Lockdown. https://www.forbes.com/sites/advisoruk/2020/10/08/mobile-phone-usesurges-during covid-lockdown/#65bdc26762df. (Accessed on 10/12/2020).

[16]Zhang, Stephen X., Jing Liu, Asghar Afshar Jahanshahi, Khaled Nawaser, Ali Yousefi, Jizhen Li, and Shuhua Sun. "At the height of the storm: Healthcare staff's health conditions and job satisfaction and their associated predictors during the epidemic peak of COVID-19." Brain, behavior, and immunity 87 (2020): 144-146.

[17]Mary, J. Senophiyah, and T. Meenambal. "Inventorisation of e-waste and developing a policy–bulk consumer perspective." Procedia Environmental Sciences 35 (2016): 643-655.

[18]Scott, R., M. Palacios, and T. Maturana. "Electronic waste-A growing concern for the health sector." Gold Book [Internet]. Río de Janeiro: Universidade do Estado do Rio de Janeiro 621 (2012): 649.

[19]Mukherjee, Avinandan, and John McGinnis. "E-healthcare: an analysis of key themes in research." International Journal of Pharmaceutical and Healthcare Marketing (2007).

[20]Zaghouani, Emna Kalai, Adel Benzina, and Rabah Attia. "ECG based authentication for e healthcare systems: Towards a secured ECG features transmission." In 2017 13th international wireless communications and mobile computing conference (IWCMC), pp. 1777-1783. IEEE, 2017.

[21]Siau, Keng, Peter B. Southard, and Soongoo Hong. "E-healthcare strategies and implementation." International Journal of Healthcare Technology and Management 4, no. 1-2 (2002): 118-131.

[22]Rahmani, Amir-Mohammad, Nanda Kumar Thanigaivelan, Tuan Nguyen Gia, Jose Granados, Behailu Negash, Pasi Liljeberg, and Hannu Tenhunen. "Smart e-health gateway: Bringing intelligence to internet-of-things based ubiquitous healthcare systems." In 2015 12th Annual IEEE Consumer Communications and Networking Conference (CCNC), pp. 826-834. IEEE, 2015.

[23]Cordeiro, Jéssica Fernanda Corrêa, Magda Fabbri Isaac Silva, Adriana Cristina de Oliveira, and Silvia Rita Marin da Silva Canini. "Biological risk related to health care waste management in home care." Rev Rene 20 (2019): 65.

[24]S. P. Paik., 'E-Waste: A Tricky and Immense Problem', Parishodh Journal. 9(3); (2020) 11931-11941

[25]Filho, Jose Rodrigues. "The Challenges of Implementing e-Health Technology for Sustainability in Brazil."

[26]Shankar, Shashank Shyam, R. Sneha, and Nalina V. SanjanaRS. "The green Internet of Things: A review." Int. J. Adv. Trends Eng., Sci. Technol. 5, no. 5 (2020).

[27]Ma, Jianmin, Yutao Li, Nicholas S. Grundish, John B. Goodenough, Yuhui Chen, Limin Guo, Zhangquan Peng et al. "The 2021 battery technology roadmap." Journal of Physics D: Applied Physics 54, no. 18 (2021): 183001

Patient Monitoring And Assistance Device

Portable Smart ECG, N.I.V. Ventilator 1Kunal Pawar, 2Rohan Gujar, 3Sameer Sumbhe

1,2,3 Electronics and Telecommunication, Vishwakarma Institute of Technology, Pune, India

ABSTRACT

We have presented a Patient monitoring and assistance system that will allow continuous monitoring of patient vital signs, assist medical personnel in making decisions, and help improve patient care. In addition, we aimed to help the patient by providing a breathing assistance device, such as a portable Non-Invasive Ventilator (NIV) This system may include devices that measure, display, and record human vital signs such as body temperature, heart rate, and ECG, as well as devices that can be modified to monitor other health-related criteria. This paper proposes a system for monitoring a patient's condition by measuring heart rate and oxygen levels. In addition, the system will monitor the patient's ECG and can be accessed remotely via the cloud.

Keywords—ECG, ventilator, medical electronics, patient monitoring.

INTRODUCTION

The Smart Devices i.e., the Internet of Things is the next big step in the health care sector where the sensors collect the data from the patients and is transmitted over a cloud-based service. Through which a certified medicinal Practitioner can monitor the patient and provide the necessary treatment plan. We have proposed for the remote assistance along with the monitoring of the patient.

The Non-invasive method in providing ventilation for the patients is better than the traditional intra nasal methods. Non-invasive ventilation (NIV) is the delivery of oxygen (supported ventilation) through a face mask without the need for an endotracheal airway. NIV achieves physiological benefits comparable to conventional ventilators by reducing the work of breathing and improving gas exchange. Studies show that non-invasive ventilation after early extubating appears to help reduce the total number of days spent on invasive ventilation. This intervention is designed to improve breathing in chronic obstructive pulmonary disease, cardiogenic pulmonary edema, and other respiratory diseases without complications such as respiratory muscle weakness, upper airway trauma, ventilator-associated pneumonia, and sinusitis. It is recognized as an effective treatment for insufficiency.Heart diseases have become a major problem in recent decades, and many people die from certain health problems. Therefore, heart disease should not be taken lightly. Therefore, there is a need for technology that can regularly monitor a patient's heart rate and heart motion.

Various heart diseases can be prevented by analysing or monitoring ECG signals in the early stages.

MOTIVATION

There is lack of research in developing an all-in-one patient monitoring device in addition to it the existing machine can't assist the patient in any way like in assisting the breathing. The recent events have opened the eyes of the healthcare sector for the need of ventilators and the remote patient monitoring devices. Due to the nature of Covid there was a need of remote monitoring of patients and also assisting them. As the virus targets the patients' lungs the patient needs to be assisted in breathing. The PMAD will make it possible for the remote monitoring and assistance of the patients.

LITERATURE SURVEY

A group of scientists published a paper on the use of electrocardiograms (ECGs) [1] to diagnose heart diseases. A health-care application based on Internet of Things (IoT) can continuously monitor individuals' ECG signals remotely over a longer time period. The main benefits of IoT in healthcare are patient monitoring, analysis, diagnosis, and control. Electrocardiograms are used to detect cardiac abnormalities by analysing small electrical impulses generated by the heart. According to AAMI guidelines, available ECG signal beats are divided into two categories: critical and non-critical.A team of researchers has developed a mobile health monitoring device [2] that alerts the patient when he is in danger of developing a heart attack or another serious health condition.

The CMS50D pulse oximeter is small, lightweight, accurate, inexpensive, and consumes very little power. When predefined warning levels are reached, the microcontroller software alerts the patient. The monitoring range is determined by the communication method used, with Bluetooth providing a short range (20 m) and wireless providing a range of up to 100 m.A team of researchers has developed [3] an e-health system that monitors oxygen levels in an airplane's cabin. Pulse oximetry is a technique for measuring blood oxygen saturation (SpO2) and pulse rate. It provides data on lung capacity to ensure that the body receives an adequate amount of oxygen even when no effort is exerted. The person can be identified thanks to the use of a pulse oximeter integrated into the SDU. The pulse oximeter measures blood oxygen saturation based on the amount of red light or infrared absorbed by oxyhemoglobin or deoxyhemoglobin.A low-cost sensor kit has been developed to help diagnose and treat novel coronavirus pneumonia and bronchitis. The rising number of coronavirus cases and deaths around the world has greatly increased the need for health surveillance, including: Researchers [4] developed a very low-cost wearable system based on the MAX30100 and tested it in 12 consenting subjects. The group found a minimum acceptable deviation of 0.8175% for pulse rate and 0.425% for SpO2. This study included 12 participants. You have indicated that there are many opportunities for further research and development. Potential applications include remote detection of Covid symptoms, mobile app-based telemedicine, and heart disease detection and analysis.

A researcher [5] used a smartphone to study the relationship between pain and weather and examined the results. Dixon and his colleagues (2019) reported that her 13,207 users downloaded the survey app during a 12-month recruitment period. A total of 10,584 had complete baseline data and at least he had one pain entry. Compared to an average day, the "worst" combination of weather variables increases the likelihood of pain occurrence by more than 20%. High relative humidity, high wind speed, and low atmospheric pressure are associated with increased pain intensity in people with chronic pain. The effect of weather on pain was not fully accounted for by its effects on mood and daily physical activity. The analysis included 2658 patients. However, the study was "advertised to participants with a clear research question," the authors write. They argue that rainy and cold weather was the prevailing belief. "Because pain reporting is subjective, participants' 'moderate' pain may correspond to 'severe' pain," the authors admit.This paper [6] seeks to apply reverse engineering concepts to the design and construction of low-cost ambulatory CPR and ventilators. According to Abdullah Al-Aubidy (2021), in 2020 the world was exposed to the coronavirus known as his COVID-19 pandemic. The main goal of this research is to design and build a ventilator using reverse engineering concepts. The virus severely impacts lung function and can lead to patient death. Hospital ventilation and cardiac resuscitation equipment is complex, expensive, and has limitations.

A group of Scottish researchers [7] have proposed an ECG signal generator that could be used to detect and treat cardiovascular diseases. The world is dealing with a high rate of heart disease. The World Health Organization (WHO) estimates that more than 17 million people die each year as a result of cardiovascular disease. A typical method for detecting heart disease or cardiovascular disease in a person is to send a diagnosis to a pathology centre and obtain an ECG signal for testing. A portable ECG signal generator circuit, a data transfer device, and a smart device comprise the system design. It has the potential to reduce deaths from heart attacks and other cardiovascular diseases.

Proposed a scheme [8] that increases the bitrate of distributed video encoding by 2.9% while also increasing the speed by 15.3% over existing schemes. Myunghoon Jeon (2016) investigated content-aware video segmentation and scheduling in map reduce-based distributed video encoding. CAET increased bitrate by 2.9% when compared to the most popular segmentation schemes in the field of distributed encoding. It improved overall performance efficiency and increased encoding speed by 15.3%. More research is needed to improve the content differentiation process's efficiency. The encoding tasks that are part of the video coding process that require a high computational complexity are distributed using distributed encoding. The bitrate, Peak Signal to Noise Ratio (PSNR), and encoding speed of distributed encoding can all vary. CAET increased bitrate by 2.9% compared to the main existing segmentation schemes, but it also increased encoding speed by 15.3% and improved overall performance efficiency. The study included four subjects. The team claims that changes in the SOI differentiation performance based on window size resulted in different results depending on the video used. As a result, more research is required to effectively set window size.

Researchers [9] trained a neural network using artificial intelligence (AI) to identify human heartbeats from electrocardiograms (ECG). At an average heart rate of 80 beats per minute, this means that one PQRST period takes 0.75 seconds. The proposed algorithm employs ECG signals that have been normalized to be based on the same heart rate. The Fourier transform technique is used to extract ECG features. The heart rates of the ECG signals used in this paper have been normalized to a standard heart rate. Using a neural network, the significant Fourier components are used in the classification process.

METHODLOGY

After carefully analysing the existing systems available on the market showed that some parameter constraints like the size i.e., bulkiness, price range, available functions, portability are of concern So the proposed system was aimed to overcome these problems.

The system is divided into Three modules for efficient working and work load distribution. The separation allows the one module to be turned off in case they are not being used. The buttons allow the modules to be operated at the user's discretion.

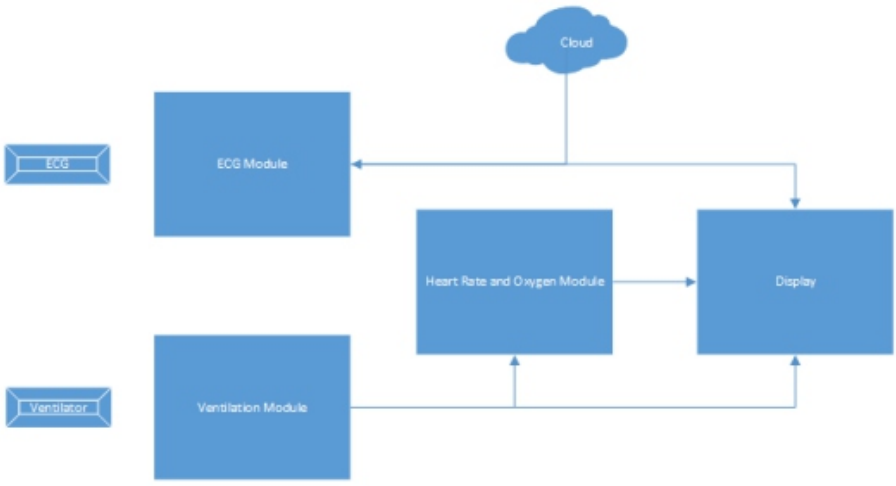

Figure 1 Proposed System Block Diagram

A. ECG Module

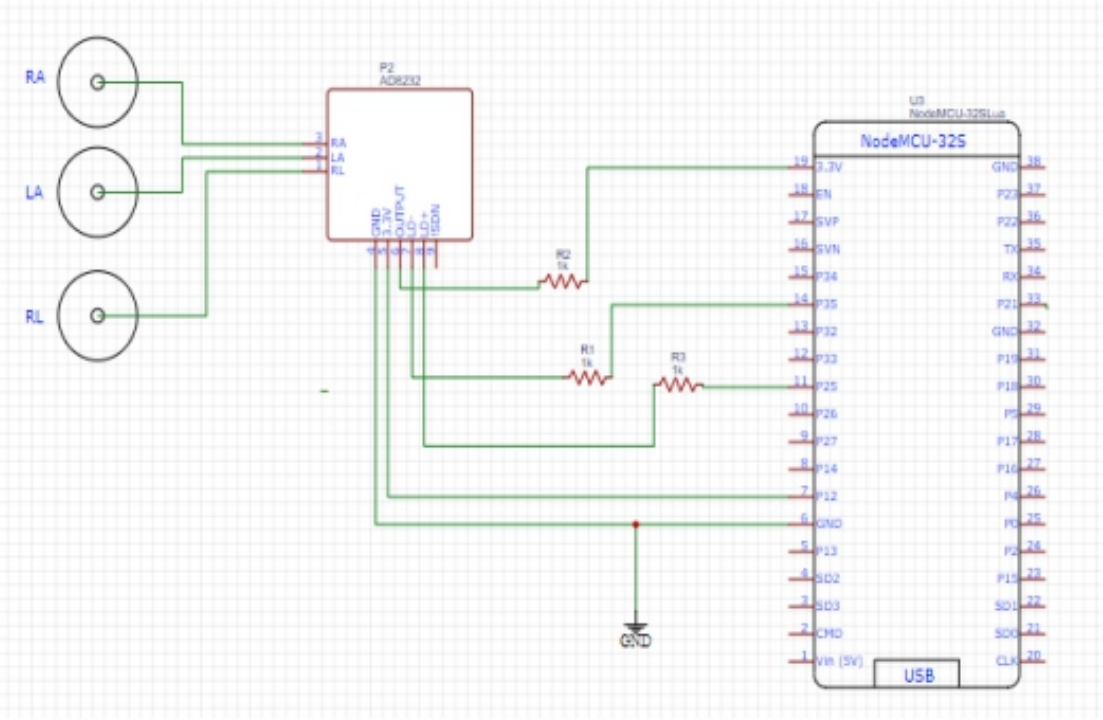

Figure 2 ECG Module

An electrocardiogram (ECG) was monitored using the AD8232 sensor. This sensor is an inexpensive circuit board that measures the heart's electrical activity. This electrical activity is recorded as an electrocardiogram and output as an analog reading. Electrocardiograms can be very noisy. The AD8232 single-channel heart rate monitor acts as an operational amplifier to easily obtain clear signals from the PR and QT intervals.

An electrocardiogram (ECG) was monitored using the AD8232 sensor. This sensor is an inexpensive circuit board that measures the heart's electrical activity. This electrical activity is recorded as an electrocardiogram and output as an analog reading. Electrocardiograms can be very noisy. The AD8232 single-channel heart rate monitor acts as an operational amplifier to easily obtain clear signals from the PR and QT intervals.

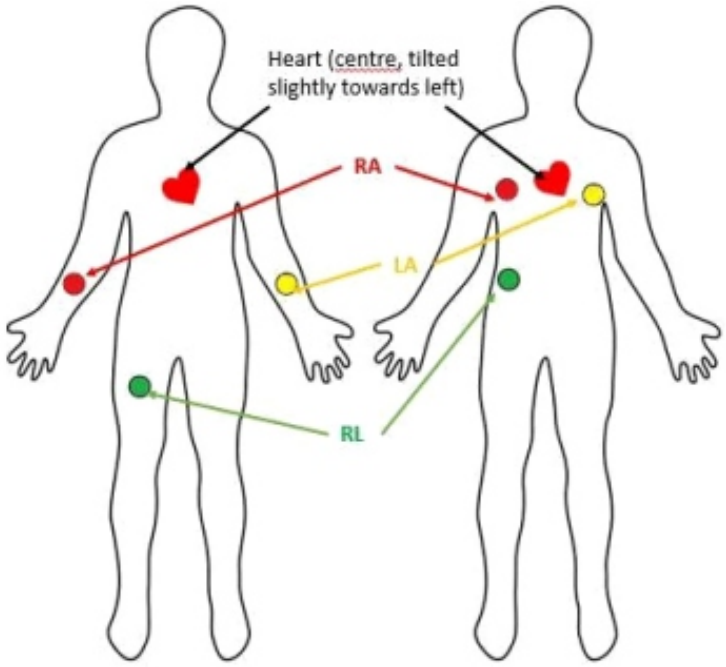

Figure 3 ECG Electrode Placement

This module will monitor the patients ECG and transmit the graph to the cloud through which any licensed medicinal practitioner anywhere in the world will be able to prescribe the necessary treatments and take the required steps. This module is designed keeping in mind the architecture of the current medical situation like the low doctor to patient ratio. Due to its remote monitoring the large sized hospitals can keep an eye on a number of patients simultaneously without compromising the patient's needs.

B. Heart Rate and oxygen Module

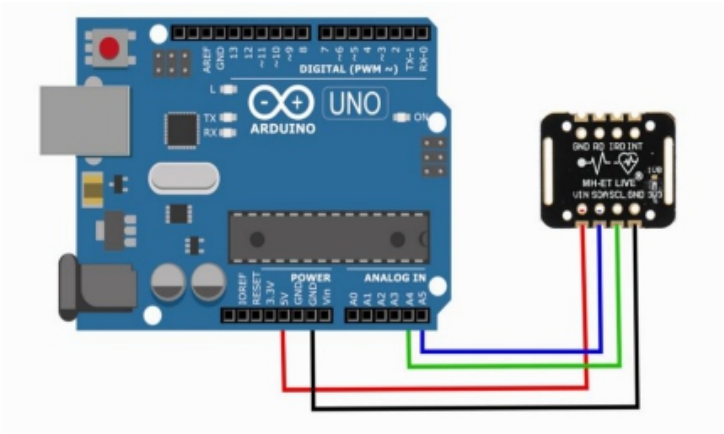

Figure 4 Pule & Oxygen Module

This module houses the blood oxygen and heart rate sensors. Pulse oximetry measures the intensity of reflected red and infrared light to monitor blood oxygen saturation. By analysing the time series response of reflected red and infrared light, a pulse oximeter can also estimate heart rate. In addition to heart rate and blood oxygen levels, the MAX30102 sensor can measure other body temperatures. This is a sensor developed by Analog Devices that includes two LEDs (one for infrared and one for red), a photodetector, optics, and a low power sensor for detecting pulse oximetry (SpO2) and heart rate (HR) signals. It has a noise signal processing unit. The main idea is that he lights up one LED at a time and sees how much light is reflected back to the sensor. Based on reflexes, blood oxygen levels and heart rate can be determined. The module is equipped with a buzzer to notify of the drop in oxygen levels and
the heart rate.

Ventilation Module

Most fluid power circuits are controlled by electrical and electronic equipment. Control schemes include relay logic, programmable controllers, and computers. Air logic is another approach to controlling pneumatic systems. All functions normally handled by relays, pressure or vacuum switches, time delays, limit switches, or counters can be performed by Air Logic Controls. The circuit is similar, but compressed air is used as the control medium instead of electricity. Air Logic controllers are ideal for humid or dusty environments. The Air logicsystem is non-explosive, shock hazard-free, and splash water will not affect control functionality. The control medium - clean compressed air - cannot be ignited in the event of an external explosion.

For full control of breathing, the board must be able to connect to high pressure, low pressure and atmospheric pressure independently. The diagram below describes a simple way to configure the pump and valves to accomplish this. Solid lines represent air tubes. There are three valves below, all closed. The inlets of the valve are connected from above to high pressure, low pressure and atmospheric pressure. All valve outputs are interconnected and connected to pressure sensors and masks.

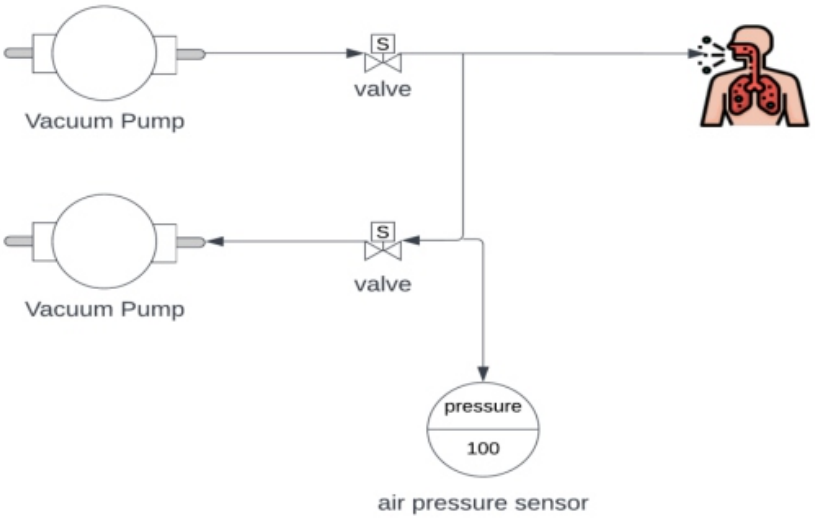

Figure 5 Ventilation Module

PROGRAM FLOW

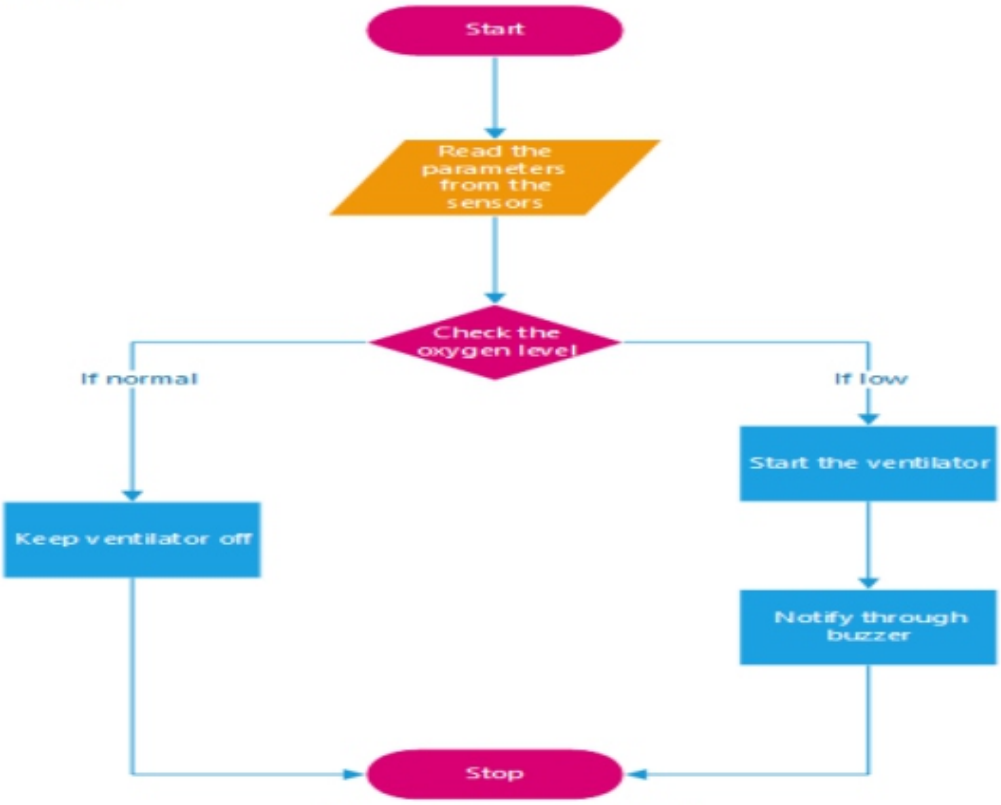

Figure 6 Program Flow 1

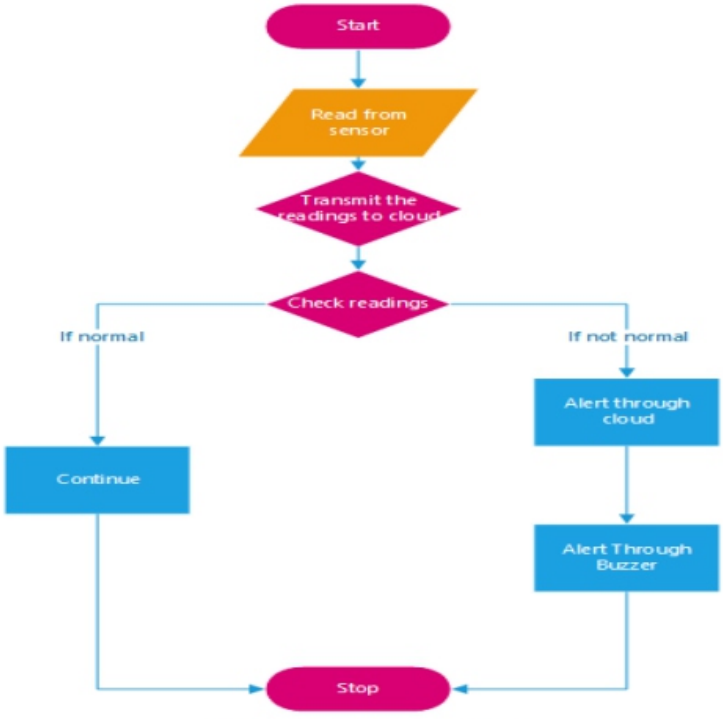

Figure 7 Program Flow 2

II. RESULTS

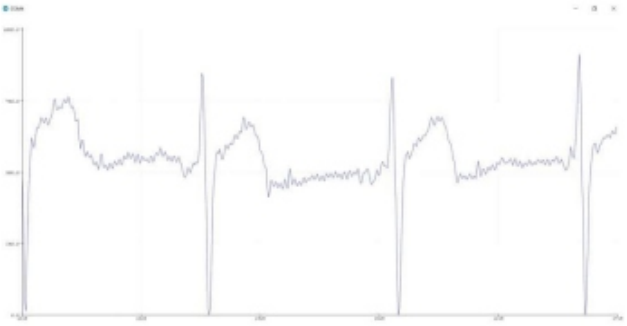

Figure 8 ECG Readings

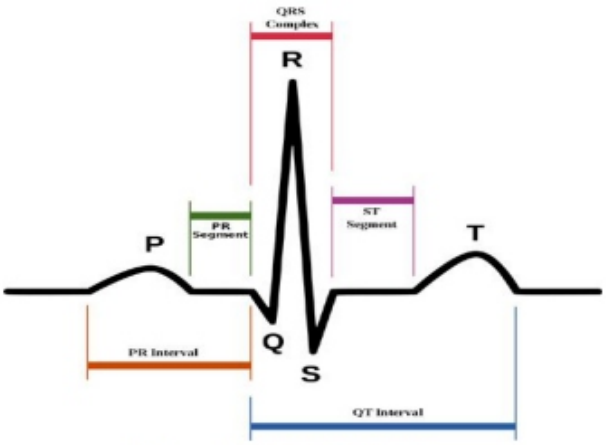

Figure 9 Ideal ECG Wave

Each interval has a range of optimal values, and deviations from this range may be associated with specific diseases. Here are the main components of the ECG signal.

1. P Wave - This is the left posterior wave of the QRS complex.
2. QRS Complex - Impulses produced by ventricular contraction.
3. T wave - This is the leading wave going directly to the QRS complex.
4. U wave - Not always observed due to low wave height.

Many heart diseases and irregularities can be diagnosed based on the shape of the above features, the intervals between them, and the intervals between them. Examples:

1. Irregular heartbeat or absence of P waves: Atrial fibrillation
2. Normal heart rate >100 = Tachyarrhythmia
3. Tachyarrhythmia and delta waves: Wolf-Parkinson-White or WPW syndrome
4. Serrated P wave: atrial flutter
5. ST segment depression: this may indicate ischemia
6. ST segment elevation: this may indicate myocardial infarction

Therefore, the ECG is It is very important for cardiologists and doctors on this subject.

Figure 10 ECG Electrode Placement on Hand

```
red=1708, ir=1862, HR=83, HRvalid=1, SPO2=95, SPO2Valid=1
red=1731, ir=1852, HR=83, HRvalid=1, SPO2=95, SPO2Valid=1
red=1727, ir=1882, HR=83, HRvalid=1, SPO2=95, SPO2Valid=1
red=1737, ir=1877, HR=83, HRvalid=1, SPO2=95, SPO2Valid=1
red=1752, ir=1882, HR=83, HRvalid=1, SPO2=95, SPO2Valid=1
red=1762, ir=1889, HR=83, HRvalid=1, SPO2=95, SPO2Valid=1
red=1763, ir=1893, HR=83, HRvalid=1, SPO2=95, SPO2Valid=1
red=1766, ir=1901, HR=83, HRvalid=1, SPO2=95, SPO2Valid=1
```

Figure 11 Heart Rate &SP02 Readings

The SPO2 i.e., the oxygen level in the patient will be continuously monitored and accordingly then the patient will be assisted in breathing through the Non-Invasive ventilator.

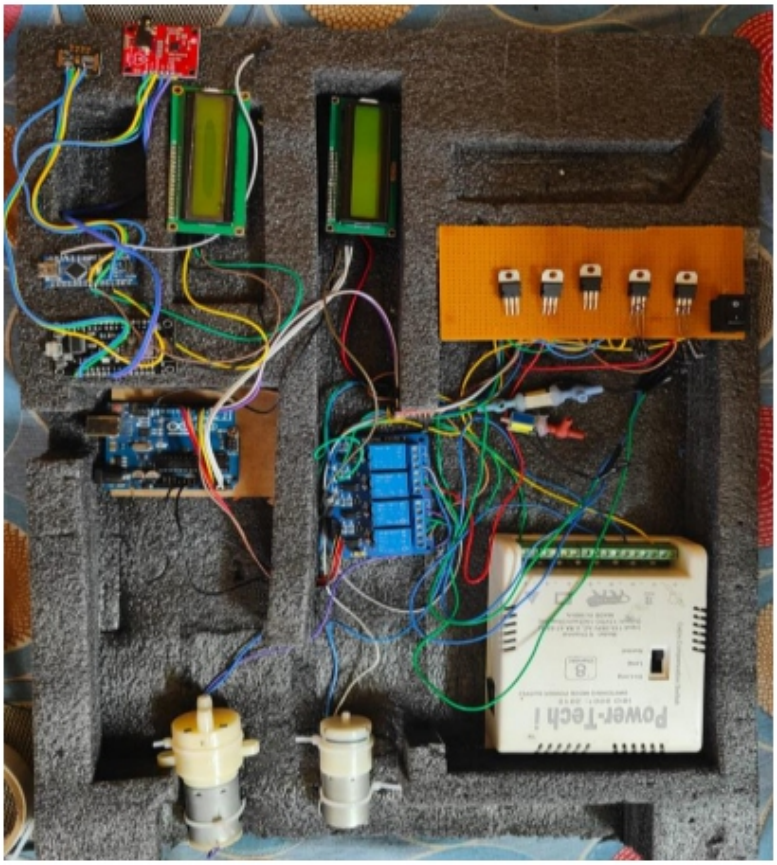

Figure 12 Proposed System

A. Post Treatment

After heavy medication and therapy, patient is suffering from difficulty breathing. In such cases, P.M.A.D. can be used.

B. Post Opertative Interventions

After invasive interventions, breathing becomes difficult, especially in the abdomen. Proper breathing after surgery is very important. Used here to support P.M.A.D respiration. It provides adequate pressure, not too high to cause barotrauma.

C. Respiratory Diseases

Respiratory diseases affect the body's ability to breathe properly. Most commonly these are associated with bacterial or viral infections. Now on takes the COVID-19 pandemic as an example, mainly dealing with people not being able to breathe normally. The lungs become infected, resulting in a decrease in important body parameters such as blood oxygen saturation. In such cases, the patient needs external support. Patients must be able to breathe properly and feel comfortable during treatment.

D. Veterinary medicine compatible

The ECG can be modified to detect the pulse waves of animals.

E. Patients Confined To Home

Patients which are confined to home treatment can be monitored efficiently through this system the doctors can monitor the patients even from their clinics also can be assisted quickly with some modifications.

FUTURE SCOPE

The proposed System can be improved through some modifications for more assistance. The Addition of a defibrator will give an advantage of correcting the sinus rhythm of heart in case of heart arrythmias remotely which can save the lives of patients. The Addition of BP monitor can improve the capacity of monitoring the patients' vitals. The ventilator can be modified to assist breathing for animals.

CONCLUSION

Keeping the purpose of designing a system to address a key in health care system, the proposed system gave us more benefits that a commercial bulky system can give. The issue of breathing ailments as well as the heart related issues still remain to save the patients' lives. The P.M.A.D. provides a cheap, fast yet an effective method of treatment in an efficient way.

Furthermore, in future the model can be improved such as miniaturized, interconnectedness through extensive collaboration with industry experts and medical professionals.

ACKNOWLEDGMENT

We would like to express my sincere gratitude towards the management of Vishwakarma Institute of Technology, Pune for their encouragement and support throughout this research work.

REFERENCES

[1]A. P. Roy, S. Chatterjee, P. Maji and H. K. Mondal, "Classification of ECG Signals for IoT-based Smart Healthcare Applications using WBAN," 2020 International Symposium on Devices, Circuits and Systems (ISDCS), 2020, pp. 1-4, doi: 10.1109/ISDCS49393.2020.9263011.

[2]P. Szakacs-Simon, S. A. Moraru and L. Perniu, "Pulse oximeter based monitoring system for people at risk," 2012 IEEE 13th International Symposium on Computational Intelligence and Informatics (CINTI), 2012, pp. 415-419, doi: 10.1109/CINTI.2012.6496802.

[3]R. M. AILENI, S. PAŞCA and A. FLORESCU, "E-Health Monitoring by Smart Pulse Oximeter Systems Integrated in SDU," 2019 11th International Symposium on Advanced Topics in Electrical Engineering (ATEE), 2019, pp. 1-4, doi: 10.1109/ATEE.2019.8724865.

[4]N. B. Ahmed, S. Khan, N. A. Haque and M. S. Hossain, "Pulse Rate and Blood Oxygen Monitor to

Help Detect Covid-19: Implementation and Performance," 2021 IEEE International IOT, Electronics and Mechatronics Conference (IEMTRONICS), 2021, pp. 1-5, doi: 10.1109/IEMTRONICS52119.2021.9422520

[5]M. J. Ghafoor, M. Naseem, F. Ilyas, M. S. Sarfaraz, M. I. Ali and A. Ejaz, "Prototyping of a cost effective and portable ventilator," 2017 International Conference on Innovations in Electrical Engineering and Computational Technologies (ICIEECT), 2017, pp. 1-6, doi: 10.1109/ICIEECT.2017.7916539.

[6]A. W. Al-Mutairi and K. M. Al-Aubidy, "Design and Construction of a Low Cost Portable Cardiopulmonary Resuscitation and Ventilation Device," 2020 17th International Multi-Conference on Systems, Signals & Devices (SSD), 2020, pp. 390-397, doi: 10.1109/SSD49366.2020.9364088.

[7]S. Deb, S. M. R. Islam, J. RobaiatMou and M. T. Islam, "Design and implementation of low cost ECG monitoring system for the patient using smart device," 2017 International Conference on Electrical, Computer and Communication Engineering (ECCE), 2017, pp. 774-778, doi: 10.1109/ECACE.2017.7913007.

[8]M. Jeon, N. Kim and B. -D. Lee, "MapReduce-Based Distributed Video Encoding Using Content-Aware Video Segmentation and Scheduling," in IEEE Access, vol. 4, pp. 6802-6815, 2016, doi: 10.1109/ACCESS.2016.2616540.

[9]S. Saechia, J. Koseeyaporn and P. Wardkein, "Human Identification System Based ECG Signal," TENCON 2005 - 2005 IEEE Region 10 Conference, 2005, pp. 1-4, doi: 10.1109/TENCON.2005.300986.

[10]Breathing Recovery Assistance Device (Brad) For Patients With Acute Respiratory Failure, Amruta Amune, Kunal Pawar, Rohan Gujar,Vishwakarma Institute of Technology, Pune, India., Page No: 352-361,DOI:20.18001.GSJ.2022.V9I12.22.40448.

Instructions for Authors

Essentials for Publishing in this Journal

1 Submitted articles should not have been previously published or be currently under consideration for publication elsewhere.

2 Conference papers may only be submitted if the paper has been completely re-written (taken to mean more than 50%) and the author has cleared any necessary permission with the copyright owner if it has been previously copyrighted.

3 All our articles are refereed through a double-blind process.

4 All authors must declare they have read and agreed to the content of the submitted article and must sign a declaration correspond to the originality of the article.

Submission Process

All articles for this journal must be submitted using our online submissions system. http://enrichedpub.com/ . Please use the Submit Your Article link in the Author Service area.

Manuscript Guidelines

The instructions to authors about the article preparation for publication in the Manuscripts are submitted online, through the e-Ur (Electronic editing) system, developed by **Enriched Publications Pvt. Ltd**. The article should contain the abstract with keywords, introduction, body, conclusion, references and the summary in English language (without heading and subheading enumeration). The article length should not exceed 16 pages of A4 paper format.

Title

The title should be informative. It is in both Journal's and author's best interest to use terms suitable. For indexing and word search. If there are no such terms in the title, the author is strongly advised to add a subtitle. The title should be given in English as well. The titles precede the abstract and the summary in an appropriate language.

Letterhead Title

The letterhead title is given at a top of each page for easier identification of article copies in an Electronic form in particular. It contains the author's surname and first name initial .article title, journal title and collation (year, volume, and issue, first and last page). The journal and article titles can be given in a shortened form.

Author's Name

Full name(s) of author(s) should be used. It is advisable to give the middle initial. Names are given in their original form.

Contact Details

The postal address or the e-mail address of the author (usually of the first one if there are more Authors) is given in the footnote at the bottom of the first page.

Type of Articles

Classification of articles is a duty of the editorial staff and is of special importance. Referees and the members of the editorial staff, or section editors, can propose a category, but the editor-in-chief has the sole responsibility for their classification. Journal articles are classified as follows:

Scientific articles:

1. Original scientific paper (giving the previously unpublished results of the author's own research based on management methods).

2. Survey paper (giving an original, detailed and critical view of a research problem or an area to which the author has made a contribution visible through his self-citation);

3. Short or preliminary communication (original management paper of full format but of a smaller extent or of a preliminary character);

4. Scientific critique or forum (discussion on a particular scientific topic, based exclusively on management argumentation) and commentaries. Exceptionally, in particular areas, a scientific paper in the Journal can be in a form of a monograph or a critical edition of scientific data (historical, archival, lexicographic, bibliographic, data survey, etc.) which were unknown or hardly accessible for scientific research.

Professional articles:

1. Professional paper (contribution offering experience useful for improvement of professional practice but not necessarily based on scientific methods);
2. Informative contribution (editorial, commentary, etc.);
3. Review (of a book, software, case study, scientific event, etc.)

Language

The article should be in English. The grammar and style of the article should be of good quality. The systematized text should be without abbreviations (except standard ones). All measurements must be in SI units. The sequence of formulae is denoted in Arabic numerals in parentheses on the right-hand side.

Abstract and Summary

An abstract is a concise informative presentation of the article content for fast and accurate Evaluation of its relevance. It is both in the Editorial Office's and the author's best interest for an abstract to contain terms often used for indexing and article search. The abstract describes the purpose of the study and the methods, outlines the findings and state the conclusions. A 100- to 250-Word abstract should be placed between the title and the keywords with the body text to follow. Besides an abstract are advised to have a summary in English, at the end of the article, after the Reference list. The summary should be structured and long up to 1/10 of the article length (it is more extensive than the abstract).

Keywords

Keywords are terms or phrases showing adequately the article content for indexing and search purposes. They should be allocated heaving in mind widely accepted international sources (index, dictionary or thesaurus), such as the Web of Science keyword list for science in general. The higher their usage frequency is the better. Up to 10 keywords immediately follow the abstract and the summary, in respective languages.

Acknowledgements

The name and the number of the project or programmed within which the article was realized is given in a separate note at the bottom of the first page together with the name of the institution which financially supported the project or programmed.

Tables and Illustrations

All the captions should be in the original language as well as in English, together with the texts in illustrations if possible. Tables are typed in the same style as the text and are denoted by numerals at the top. Photographs and drawings, placed appropriately in the text, should be clear, precise and suitable for reproduction. Drawings should be created in Word or Corel.

Citation in the Text

Citation in the text must be uniform. When citing references in the text, use the reference number set in square brackets from the Reference list at the end of the article.

Footnotes

Footnotes are given at the bottom of the page with the text they refer to. They can contain less relevant details, additional explanations or used sources (e.g. scientific material, manuals). They cannot replace the cited literature.
The article should be accompanied with a cover letter with the information about the author(s): surname, middle initial, first name, and citizen personal number, rank, title, e-mail address, and affiliation address, home address including municipality, phone number in the office and at home (or a mobile phone number). The cover letter should state the type of the article and tell which illustrations are original and which are not.

Address of the Editorial Office:

Enriched Publications Pvt. Ltd.
S-9,IInd FLOOR, MLU POCKET,
MANISH ABHINAV PLAZA-II, ABOVE FEDERAL BANK,
PLOT NO-5, SECTOR -5, DWARKA, NEW DELHI, INDIA-110075,
PHONE: - + (91)-(11)-45525005

Note